



FRONTIER LETTER

Open Access



A brief review of single silicate crystal paleointensity: rock-magnetic characteristics, mineralogical backgrounds, methods and applications

Chie Kato^{1*} , Yoichi Usui² and Masahiko Sato^{3,4} 

Abstract

Single silicate crystals hosting tiny magnetic inclusions are remarkable targets to study the paleointensities of the Earth and extraterrestrial samples. Since the pioneering work done in late 1990s, paleointensity studies using various silicate minerals such as feldspar, quartz, zircon, pyroxene, and olivine with magnetic inclusions trapped during grain growth or exsolved from the host phase have been reported. It has been shown that some single crystals have the ability to record paleomagnetic information as reliable or more reliable than the whole rock, by direct comparison of the obtained paleointensity estimate from single crystal and the whole-rock sample or the magnetic observatory data. Various rock-magnetic studies also support the fidelity of these crystals. Here, we provide a brief review of the rock-magnetic characteristics of the single crystals, the mineralogical background of the hosting silicates, and experimental procedures developed to obtain reliable data from magnetically weak samples with distinctive rock-magnetic features. We also overview the studies on paleointensity and related topics on various terrestrial and extraterrestrial samples published mainly after the comprehensive reviews in late 2000s. The present review covers the advantages as well as the limitations and caveats of paleointensity studies using single crystal samples and will help readers who wish to utilize this technique in their research.

Keywords Paleointensity, Single crystal, Magnetic inclusion, Exsolution

*Correspondence:

Chie Kato

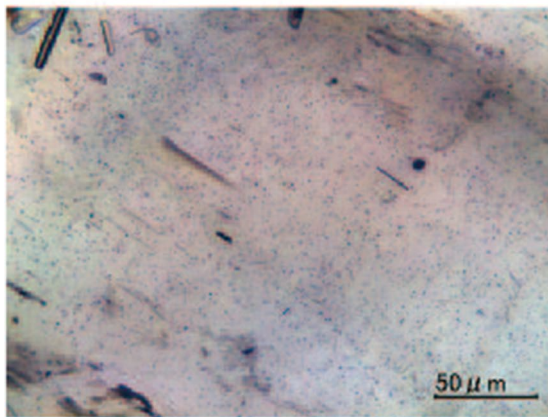
c.kato@scs.kyushu-u.ac.jp

Full list of author information is available at the end of the article

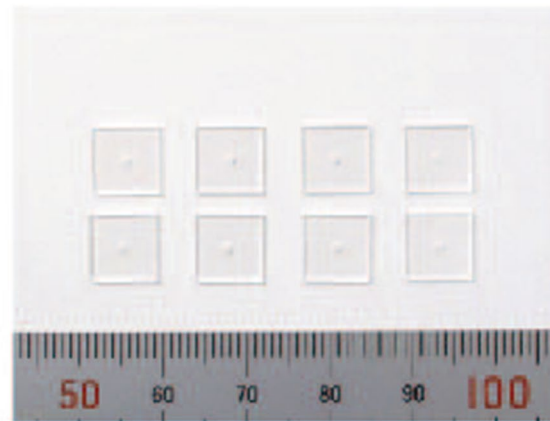


© The Author(s) 2024. **Open Access** This article is licensed under a Creative Commons Attribution 4.0 International License, which permits use, sharing, adaptation, distribution and reproduction in any medium or format, as long as you give appropriate credit to the original author(s) and the source, provide a link to the Creative Commons licence, and indicate if changes were made. The images or other third party material in this article are included in the article's Creative Commons licence, unless indicated otherwise in a credit line to the material. If material is not included in the article's Creative Commons licence and your intended use is not permitted by statutory regulation or exceeds the permitted use, you will need to obtain permission directly from the copyright holder. To view a copy of this licence, visit <http://creativecommons.org/licenses/by/4.0/>.

Graphical Abstract



Magnetite inclusions in plagioclase



Glass plate holders for single silicate crystals

Introduction

The strength of the geomagnetic field is an important characteristic throughout the history of the Earth, which is related to the activity of the liquid core (e.g., Olson and Christensen 2006) and affects the surface environment via the interaction with the solar wind (e.g., Tarduno et al. 2014). Paleointensity can be estimated by comparing the strength of the natural remanent magnetization (NRM) of geologic samples to those acquired in a known field in the laboratory. However, such attempts are often hampered by various matters, and obtaining reliable data is challenging.

The alteration of magnetic minerals that has occurred in nature and may occur during laboratory heating is a critical issue in paleointensity experiments. Several experimental protocols have been designed to detect and to correct for the thermal alteration during heating and other non-ideal behavior of the magnetic particles (e.g., Coe 1967; Tsunakawa and Shaw 1994; Yamamoto et al. 2003; Tauxe and Staudigel 2004). However, the older the sample, weathering and other alteration in nature tends to become more severe and samples that are suitable for paleointensity estimate get rarer. Another issue is that the rock-magnetic properties of the samples are not always appropriate for recording paleomagnetic information over geological times. Intrusive rocks are important targets especially for studying older ages, but often contain coarse-grained magnetite that are magnetically unstable and show an undesirable behavior during the paleointensity measurements.

One approach to extend the range of samples for paleointensity study is to extract a portion that

contains magnetically and chemically stable magnetic particles exclusively. Single silicate crystal paleointensity (SCP) is a procedure which separates single crystals of rock-forming silicate minerals containing tiny magnetic inclusions and use them for paleointensity experiments (Cottrell and Tarduno 1999; Tarduno et al. 2006; Tarduno 2009). By selecting appropriate crystals, one can obtain samples containing only single domain (SD) and/or pseudo single domain (PSD) magnetite, avoiding multi domain (MD) particles. They are less susceptible to thermal alternation in nature and during laboratory heating as the magnetic particles are encapsulated in the host mineral. Another significant advantage of this method is that the most suitable specimens can be selected from a large number of candidates even with different mineralogy, from a piece of a rock of the same size as a conventional whole-rock sample.

Reliability of the SCP method has been checked by comparing the obtained paleointensity value to the observed value at the age when the sample was formed, and to those from the bulk sample of the same rock. Cottrell and Tarduno (1999) conducted SCP experiments on single plagioclase crystals separated from a basalt flow in Kilauea, Hawaii erupted in 1955 and showed that the obtained value agrees with the value recorded at the Honolulu Magnetic Observatory nearby and that reported from whole-rock samples of the same locality. They also demonstrated that single plagioclase crystals give more reliable estimate than the whole rock in the case of the Rajmahal Trap basalts (113–115 Ma, India) which contain clay minerals in the groundmass and are prone to thermal alteration during laboratory

heating (Cottrell and Tarduno 2000). Sato et al. (2015a) showed that selected zircons in fluvial sands collected in the Tanzawa plutonic complex, Japan (ca. 5 Ma; Tani et al. 2010), yield paleointensity consistent with the age of the base rocks by a simple NRM/thermoremanent magnetization (TRM) experiment. Using the Bishop tuff (767.1 ka, USA), Fu et al. (2017) reported that zircons can retain a mean paleointensity value roughly consistent to that from the whole rock (Gee et al. 2010), after excluding data from possible maghemite-bearing grains. For intrusive rocks, Kato et al. (2018) showed that single plagioclase crystals with exsolved magnetite separated from the Iritono granite (115 Ma, Japan) recorded paleointensity comparable to that from the whole rock (Tsunakawa et al. 2009) (Fig. 1). Rock-magnetic studies including magnetic hysteresis, first-order reversal curves (FORC) diagrams and low-temperature magnetometry support that these single crystal samples are magnetically stable recorders of the ancient field (e.g., Cottrell and Tarduno 1999; 2000; Tarduno et al. 2002; 2006; 2007; 2010; 2012; 2021; Smirnov et al. 2003; Tarduno and Cottrell 2005; Cottrell et al. 2008; Tarduno 2009; Usui and Nakamura 2009; Muxworthy and Evans 2012; Bono and Tarduno 2015; Sato et al. 2015a, b; Usui et al. 2015; Usui and Tian 2017; Kato et al. 2018; Bono et al. 2019a, b; Nakada et al. 2019; Zhou et al. 2022). Studies have shown the higher dominance of SD and/or PSD particles in single crystal samples in comparison to the whole rock, especially in intrusive rocks (e.g., Tarduno et al. 2002; 2006; 2007; 2010; Smirnov et al. 2003; Tarduno and Cottrell 2005; Wakabayashi et al. 2006; Cottrell et al. 2008; Tarduno 2009; Bono and Tarduno 2015; Usui et al. 2015; Kato et al. 2018; Zhou et al. 2022). Therefore, a reliable paleointensity value

may be obtained by SCP technique even if a whole-rock sample is not suitable for paleomagnetic investigations. In summary, it has been shown that in various samples single crystals are reliable recorders of paleointensity, comparable to or better than the whole rock.

The SCP was developed by Cottrell and Tarduno (1999) and has been actively carried out by their group. The achievements in the first decade and outlook for the future are documented in two review articles by Tarduno et al. (2006) and Tarduno (2009). Tarduno et al. (2006) provided a comprehensive review of early studies on mineralogy, techniques, obtained paleointensity data, and the significance in Earth and planetary sciences. They also presented a vision for study areas in the future, including application to Archean and older rocks and detrital zircons to reveal the early history of the geodynamo, potential and caveats of intrusive rocks and exsolved magnetic minerals, and studies of extraterrestrial samples. The subsequent review by Tarduno (2009) described updates including application to Precambrian Earth and use of oriented samples.

Now, SCP and related studies have been conducted by several research groups, and there have been many advances in the mineralogical background and improvements in measurement techniques, as well as new paleointensity data since the publication of the above reviews. This article aims to provide a guide on mineralogy of the studied samples and experimental techniques for readers interested in this field. We also overview the geophysical achievements of SCP studies on both terrestrial and extraterrestrial samples. The topics presented here are mainly from studies published after Tarduno et al. (2006) and Tarduno (2009), although there are some overlap due to the nature of a review.

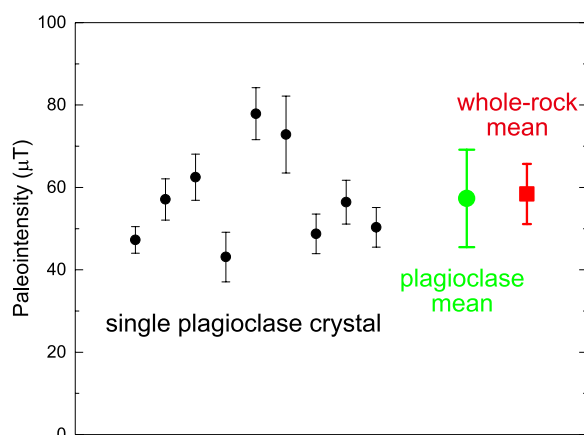


Fig. 1 Paleointensity from single plagioclase crystals compared to those from whole-rock samples. Reproduced from Fig. 11 in Kato et al. (2018)

Characteristics and mineralogical backgrounds of various silicate minerals used in paleointensity studies

Paleointensity estimate requires information on the origin of the magnetic record of the sample (i.e., type of remanence, (un)blocking temperature, and cooling rate) and how it is recorded (e.g., remanence anisotropy of the sample) for selecting appropriate samples to study and properly interpreting the results obtained. These aspects are intimately linked to the origin of the magnetic minerals that carry the remanence of the sample.

There are at least two contrasting origins of the magnetic particles that carry the magnetization of single silicate grains; one is the incorporation into the host mineral during its crystallization and the other is the exsolution from the host phase (Tarduno et al. 2006). The former can take place for any mineral kind in principle, while the latter occurs in feldspars, pyroxenes, amphibole, olivine,

and perhaps other minerals. If the magnetic inclusions are xenocrysts trapped during magmatic crystallization of the host phase, they were most likely formed at temperatures well above its Curie point, and magnetic anisotropy is generally not a severe concern. Therefore, the process of remanence acquisition and interpretation of the results of paleomagnetic measurements are straightforward. On the other hand, a large number of samples need to be screened to select those with suitable magnetic properties for paleointensity experiments. One should exclude those with insufficient magnetization or those containing coarse-grained, magnetically unstable particles (Tarduno et al. 2006). If the magnetic inclusions are exsolved magnetite, the situation might be more complex. Exsolution of magnetite sometimes (but not always) results in preferred orientation of long needles causing strong magnetic anisotropy, and requires specific treatment considering it upon paleomagnetic investigations. In addition, if crystallization/crystal growth of the exsolved magnetite occurred at temperatures lower than the Curie point, the sample have acquired thermochemical remanent magnetization (TCRM) and it is difficult to estimate an accurate paleointensity (e.g., Dunlop and Özdemir 1997; Smirnov and Tarduno 2005). On the other hand, fine and acicular magnetite dispersed in the host silicate mineral result in high coercivity (Tarduno et al. 2006); this nature makes it a suitable paleomagnetic recorder.

In the following subsections, we overview the magnetic characteristics of silicate crystals used in SCP and related studies, and discuss the issues related to exsolved magnetite.

Minerals employed in SCP and related studies, and their magnetic carriers

Plagioclase feldspar in basalt lava was the first mineral employed in SCP studies (Cottrell and Tarduno 1999). Large plagioclase phenocrysts up to few millimeters in diameter grown in the magma chamber containing SD to PSD like magnetite inclusions are suited for isolating single crystals and paleomagnetic measurements. Feldspars are contained in a wide range of igneous rocks, and thus, most frequently used in SCP studies (e.g., Cottrell and Tarduno 1999; 2000; Tarduno et al. 2001; 2002; 2007; 2021; Tarduno and Cottrell 2005; Smirnov et al. 2003; Cottrell et al. 2008; Usui and Nakamura 2009; Kato et al. 2018; Bono et al. 2019a; Zhou et al. 2022). Note that some of these studies were on feldspar grains with xenocrystic magnetite, and the others were on grains with exsolved magnetite as a dominant magnetic carrier. Feldspars are relatively easy to be weathered and transformed into altered minerals such as clay minerals. Nonetheless, they

are suitable in studies on relatively young volcanic rocks and well-preserved intrusive rocks.

Quartz is also a candidate for SCP studies especially for old acidic rocks since it is a major constituent of crust-forming rocks and is resistant against weathering. To avoid difficulties caused by MD magnetic particles, crystals that do not show visible inclusions under the microscope should be selected (Tarduno et al. 2007). The magnetic carrier of such clean quartz crystals is confirmed to be magnetite in SD to PSD state, based on magnetic hysteresis and low-temperature magnetometry (Tarduno et al. 2007; 2010; Kato et al. 2018).

Zircon is a distinctive target due to its ability of U–Pb dating by single grain and its chemical and mechanical sturdiness. Owing to these advantages, zircon is the only mineral for which paleointensity has been reported from single detrital grains (Tarduno et al. 2015; 2020; 2023). The oldest reported paleointensity dates back to 4.2 Ga from zircons from the Jack Hills, Western Australia (Tarduno et al. 2015). For those extremely old samples that experienced a complex history of reheating and alteration, careful assessment of the age of magnetization acquisition is necessary (see 4.1. Terrestrial samples). The Jack Hills zircons contain both primary and secondary magnetic mineral inclusions, as revealed by extensive microscopic investigations (e.g., Tarduno et al. 2015; 2020; Weiss et al. 2018; Tang et al. 2019; Taylor et al. 2023). Like in many cases of ancient rocks and crystals, care must be taken to distinguish magnetizations held by primary and secondary magnetic particles. Pre-screening of zircon crystals to avoid cracks and obvious alteration features can minimize the risk, as secondary magnetic minerals reside in cracks (Tarduno et al. 2015; 2020; 2023; Borlina et al. 2020). If secondary magnetic minerals are identified, it is important to determine if they disrupt the primary remanence. For example, oxyhydroxides formed by weathering have low (<130 °C) unblocking temperatures and are easily removed during the initial stages of thermal demagnetization, and secondary magnetite particles with insufficient grain size and number of particles do not hold a stable remanence (Tarduno et al. 2020).

Pyroxenes are also present in various igneous rocks, and have been utilized for SCP and related paleomagnetic studies in both terrestrial (Muxworthy and Evans 2012; Bono et al. 2019a) and extraterrestrial (Tarduno et al. 2021) samples. Bono et al. (2019a) studied paleointensity on both plagioclase and clinopyroxene from the same Septîles intrusive suite anorthosite sample (~565 Ma) and obtained comparable results, while the NRM intensities of the clinopyroxene grains were 1 to 3 orders of magnitude greater than those of feldspars. Studies on the mechanism and temperature of magnetite

exsolution in pyroxenes are also reported (see 2.2. Mineralogical background and rock-magnetic features of crystals with exsolved magnetite).

For terrestrial samples, olivine has not been used for SCP studies due to the low tolerance for alteration which produces secondary magnetite. On the other hand, olivine crystals in extraterrestrial samples have been used for the SCP studies (Tarduno et al. 2012; Fu et al. 2014; Borlina et al. 2021). The olivine crystals in the pallasite meteorites and chondrules do not suffer from severe alteration and these crystals contain pristine fine-grained metals, which are suitable paleomagnetic recorders (see 4.2. Extraterrestrial samples).

The ‘inverse microconglomerate test’ was developed and performed on the chrome mica fuchsite grains from the Jack Hills (Cottrell et al. 2016). Fuchsite is a metamorphic mineral and the magnetic carriers were indicated to be relict Fe–Cr spinel inclusions by scanning electron microscope (SEM) and energy dispersive X-ray spectroscopy (EDS) analyses. The unblocking temperature of the fuchsite grains was between ~270 and 340 °C, lower than the peak metamorphic temperature of the area, and thus, the paleomagnetic record of those grains aid in an understanding of the histories of metamorphic reheating and deformation (see 4.1. Terrestrial samples).

Mineralogical background and rock-magnetic features of crystals with exsolved magnetite

Exsolution is the precipitation of an over-saturated component which occurs when the solubility of, in this case, iron in the host phase decreases due to changes in thermodynamic conditions, typically, decrease in temperature. Since the exsolution and the grain growth of the exsolved phase at sub-solidus conditions are time consuming, exsolved magnetite is an important magnetic source in intrusive rocks rather than in volcanic rocks (Tarduno et al. 2006). In some cases, exsolved magnetite in silicate crystals is the main carrier of the stable remanence component of the whole rock (e.g., Wakabayashi et al. 2006; Muxworthy et al. 2013; Usui 2013).

Exsolved magnetite often develops as needles or plates along specific crystallographic orientations of the host mineral (e.g., Fleet et al. 1980; Davis 1981; Feinberg et al. 2004; Wenk et al. 2011; Bono and Tarduno 2015; Usui et al. 2015; Ageeva et al. 2017; Bian et al. 2021; Zhou et al. 2022). Figure 2 shows an example of a plagioclase grain with exsolved magnetite rods. Such textures are expected to form to minimize the elastic strain energy derived from macroscopic misfit and the interfacial energy that comes from lattice mismatch at the phase boundaries (e.g., Ageeva et al. 2020). In terms of paleomagnetic studies, strong shape anisotropy arising from such mineralogical structure results in high coercivity, while very

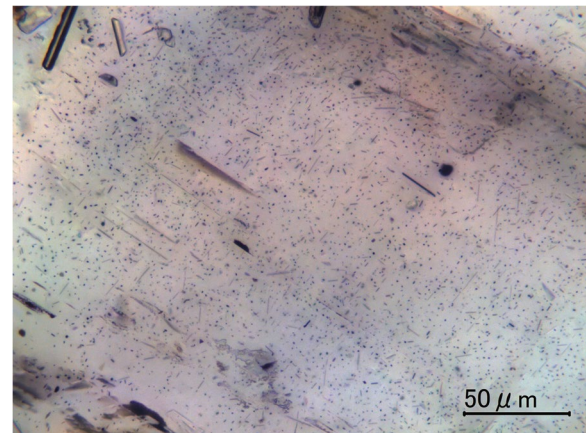


Fig. 2 Microscopic image of a plagioclase crystal extracted from the Iritono granite, Japan. Snaps of different focal depths are stacked. From Fig. 7 in Kato et al. (2018)

strong remanence anisotropy requires special treatment upon reconstruction of paleointensity and paleodirection (Feinberg et al. 2006; Usui and Nakamura 2009; Usui et al. 2015). However, this is not always the case; plagioclase and clinopyroxene crystals in some anorthosites have very fine needles with minor net anisotropy as demonstrated by TRM anisotropy experiments (e.g., Bono et al. 2019a; Zhou et al. 2022). Typical rock-magnetic features common to plagioclase and pyroxene with exsolved magnetite is the presence of distinct Verwey transition (Usui and Nakamura 2009; Sato et al. 2015b; Kato et al. 2018; Nakada et al. 2019) and FORC diagrams showing a narrow horizontal ridge along the horizontal axis (Muxworthy et al. 2013; Sato et al. 2015b; Usui et al. 2015; Zhou et al. 2022), indicating that the exsolved magnetite particles are low-Ti, well-crystallized, and non-interacting SD grains or PSD grains with nonuniform magnetization such as vortex states (Fig. 3). Therefore, plagioclase and pyroxene with exsolved magnetite could be highly stable recording media of the ancient field.

The temperature at which the magnetite inclusions were formed is critically important in estimating paleointensity since it affects whether the remanence was purely thermal or influenced by chemical processes (Tarduno et al. 2006). Current paleointensity methods assume TRM, and only the lower limit of the field intensity can be obtained if the sample had acquired a TCRM (e.g., Dunlop and Özdemir 1997; Smirnov and Tarduno 2005). The formation of remanence-carrying particles can be divided into two steps: exsolution from the host phase and decomposition of the exsolved titanomagnetite into low-Ti magnetite and ulvöspinel or ilmenite (Feinberg et al. 2005; Bian et al. 2021). For clinopyroxene, titanomagnetite exsolution from

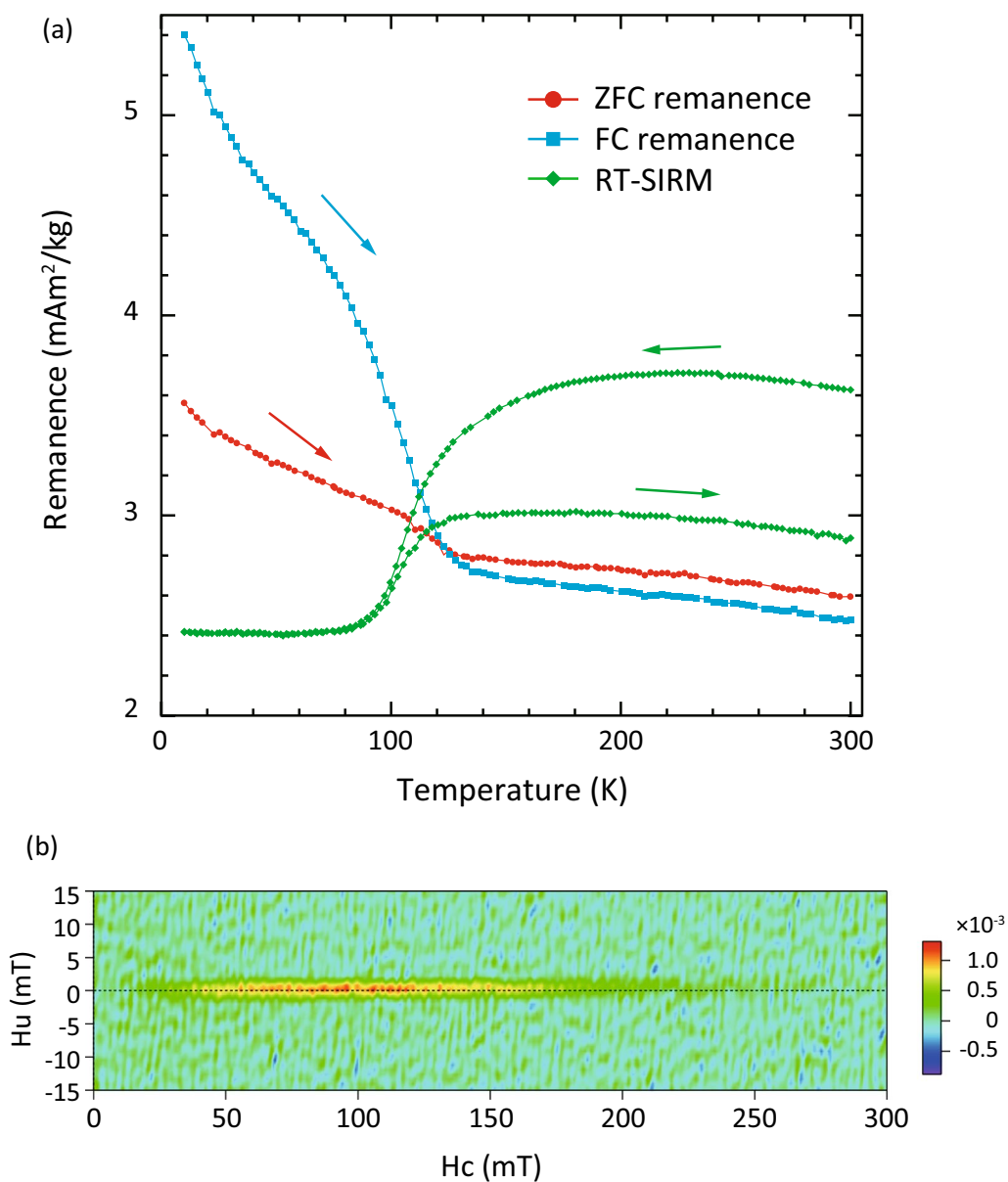


Fig. 3 Rock-magnetic measurements of a plagioclase sample from a layered gabbro from the southern part of the Oman ophiolite (Sumail massif; 23.47°N, 58.19°E). **a** Low-temperature measurements. Red circles, blue squares, and green diamonds show thermal demagnetization during zero-field warming (ZFW) for an isothermal remanent magnetization (IRM) imparted in a field of 2.5 T at 10 K after zero-field cooling from 300 K (ZFC remanence), thermal demagnetization during ZFW for a remanence given by field cooling from 300 to 10 K in a field of 2.5 T (FC remanence), and low-temperature demagnetization (LTD) cycle for saturation IRM (SIRM) imparted in a field of 2.5 T at 300 K (RT-SIRM), respectively. **b** The FORC diagram calculated using a smoothing factor of 3. From Fig. 1 in Sato et al. (2015b)

the host phase was estimated to occur at 540 ± 25 °C in ultramafic rocks from the Duke Island Complex, Alaska (Bogue et al. 1995), and at approximately 850 °C in gabbros from the Messum Complex, Namibia (Feinberg et al. 2004), as already reviewed by Tarduno et al. (2006). Although such an estimation tool has not been established for plagioclase, the exsolution temperature is considered to be high since the solubility of Fe

in plagioclase decreases with decreasing temperature (Feinberg et al. 2005).

The exsolved titanomagnetite sometimes decomposes into fine lamellae of low-Ti magnetite and ulvöspinel. The decomposition has a non-negligible impact on paleomagnetic studies; coercivity increases by decreasing magnetic grain size and the possibility of TCRM acquisition raises. Lamellae of ilmenite and/or ulvöspinel in exsolved

magnetite needles and plates have been found in various lithologies (e.g., Feinberg et al. 2005; Wenk et al. 2011; Ageeva et al. 2017; Bian et al. 2021). The temperature at which the lamellae formed can be constrained from the mineral/chemical composition, texture, and mineralogical relationship with the host magnetite. Feinberg et al. (2005) found a boxwork texture where magnetite is segmented by ulvöspinel lamellae in the interior of the exsolved titanomagnetite in the Messum clinopyroxenes. They argued that magnetic ordering at the Curie point (~ 500 °C) promoted the unmixing to magnetite and ulvöspinel (Burton 1991; Ghiorso 1997), and the magnetite with higher Curie point (~ 550 °C) acquired TCRM. Bian et al. (2021) studied plagioclase hosted magnetite micro-inclusions from oceanic gabbro dredged at the mid-Atlantic ridge, which contained oriented lamellae of ilmenite. Based on the abundance, shape, and size of the ilmenite lamellae, they concluded that it was formed at temperatures above ~ 600 °C via either the oxidation-exsolution of the Fe_2TiO_4 component in Ti-rich magnetite, or direct exsolution from non-stoichiometric magnetite.

SCP study would be greatly facilitated if we could know the rock samples containing the suitable silicate crystals for SCP study on the basis of petrologic information. The exsolution of magnetite should be related to the cooling rate, iron content, and oxygen fugacity. The crystallization and grain growth of exsolved magnetite at sub-solidus temperature is a slow phenomenon, and the rock with a slow cooling rate at around sub-solidus temperature should contain a significant amount of exsolved magnetite. The rock with a high iron content tends to contain exsolved magnetite, because a lot of iron partitions into plagioclase and the iron content in plagioclase crystal exceeds its solubility at lower temperature. These conditions are likely reflected in the fact that plagioclase grains suitable for SCP study are more common in gabbros than in basalts and granites. The oxygen fugacity conditions should have a significant role on the amount and shape of exsolved magnetite. Higher oxygen fugacity during crystallization and grain growth increases the partitioning of Fe into plagioclase (Sugawara 2001). The diffusivity of Fe ion in plagioclase relates to oxygen fugacity because of the higher diffusivity of Fe^{2+} compared to Fe^{3+} in plagioclase (Behrens et al. 1990). Moreover, the solubility of iron in the plagioclase at around sub-solidus temperature should relate to the valence state of iron. Nakada et al. (2019) compared the total Fe and $\text{Fe}^{2+}/\Sigma\text{Fe}$ of plagioclase samples from two mafic-plutonic rocks; gabbroic anorthosite FC1 in the Duluth complex (USA) which have significant amount of exsolved magnetite, and a medium-grained gabbro MT-08-206 from the Murotomisaki gabbroic intrusion (Japan) which was

practically non-magnetic. They revealed that the total Fe was higher in the MT-08-206 plagioclase and that the $\text{Fe}^{2+}/\Sigma\text{Fe}$ ratio was higher in FC1 plagioclase, suggesting that the diffusivity of iron may affect the effective amount of Fe available for exsolution. Bian et al. (2021) noted that partial reduction of Fe^{3+} and extraction of oxygen from the plagioclase is necessary to form exsolved magnetite, which may have occurred in their studied samples via interaction with reducing fluids associated with the serpentinization of ultramafic rocks. Further understanding of the mechanism of exsolution will help us to predict which intrusive rocks contain single crystals suitable for SCP studies, but currently we are far from it.

Experimental techniques for SCP studies

The magnetization of single silicate minerals is several orders of magnitude weaker than that of conventional whole-rock samples. Therefore, it is important to reduce the magnetic contamination and increase the sensitivity of the equipment to obtain credible results. In addition, some of the single crystals show large magnetic anisotropy that require specific consideration and protocols to assess and correct the effects of anisotropy of remanence and non-linear in remanence acquisition. In this section, we review the experimental techniques and protocols adopted following the procedures of SCP studies.

Field sampling strategies and screening procedures

Unfortunately, there is currently no established method to predict which rocks contain crystal grains suitable for SCP. Therefore, the basic strategy to conduct sampling over a wide area should be employed, considering the age and the thermal and/or metamorphic history. One should seek for unaltered crystals using hand lenses in the field and higher power microscopes in the lab. It is well established that alteration can occur on < 1 to > 10 m or greater scales, whereas small domains can retain fresh crystals. Since the existence/absence of crystals containing magnetic minerals and their magnetic mineral composition likely vary in meter scales even in a single intrusive unit, a screening based on pilot samples is important to narrow down the potential sampling sites.

Rock samples generally contain multiple types of silicate minerals, and thus, there are a large number of candidate silicate minerals for all sampling sites. An efficient screening of sampling sites and/or mineral types suitable for paleomagnetic investigations is absolutely essential prior to the systematic paleointensity experiments which takes time and effort. There are two main points to be screened at this stage: strength of the magnetic moment and the rock-magnetic properties such as the magnetic mineral composition and magnetic grain size distribution.

The lower bounds of recordable magnetizations are derived from a fundamental assumption of paleomagnetism that a sample contains a sufficient number of magnetic particles for statistical thermodynamics (Maxwell–Boltzmann statistics) to be met. Berndt et al. (2016) calculated the number of magnetic particles in a specimen required from this perspective, and concluded that a TRM of 10^{-11} Am² is needed for the 1% confidence limit for paleointensity and 1° confidence limit for α_{95} of paleodirection. Note that this value should be compared to the change in magnetization where the paleointensity estimates are made, but not the initial (total) NRM. Following the assumptions of Berndt et al. (2016), a relatively large statistical error should be considered in addition to errors from other sources when the magnetization of the sample is smaller than 10^{-11} Am². These potential errors can be identified and if present addressed by measurements on multiple samples collected following standard paleomagnetic sampling methods (e.g., Tarduno et al. 2002; Bono et al. 2019a; Zhou et al. 2022). Another consequence of the Maxwell–Boltzmann constraints is that a small number of secondary magnetic particles are unlikely to retain a coherent magnetization, disrupting the primary signal of a crystal.

Magnetic hysteresis can be measured for single silicate crystals using an alternating gradient magnetometer (AGM) or a magnetic property measurement system (MPMS), and is powerful and convenient for rock-magnetic screening of mineral types to use in paleomagnetic investigations (e.g., Tarduno et al. 2006; 2007; Kato et al. 2018). FORC diagrams of single silicate crystals can be measured using the AGM, and are employed to investigate the magnetic domain state distribution and magnetic interaction. Low-temperature magnetometry using the MPMS is a strong tool to check the magnetic mineral composition and dominant magnetic domains of single silicate crystals (e.g., Sato et al. 2015a; Kato et al. 2018). The Verwey transition at ~120 K is an indicator of low-Ti, well crystalline magnetite (Özdemir et al. 1993; Moskowitz et al. 1998), and monoclinic pyrrhotite (Fe₇S₈) can be detected by the presence of the Besnus transition (Bensus and Meyer 1964; Dekkers et al. 1989; Rochette et al. 1990) at ~30 K. Comparison of the strength of field-cooled (FC) remanence acquired by cooling the sample in high DC field to low temperature and zero-field-cooled (ZFC) remanence acquired by cooling the sample in zero field and applying high DC field at low temperature provides information on grain size; FC remanence larger than ZFC remanence indicate the dominance of SD and fine-grained PSD magnetite (Moskowitz et al. 1993; Carter-Stiglitz et al. 2001; 2002; Kosterov 2003). Direct observation by SEM and chemical analysis by EDS are helpful to understand the mineralogy and morphology

of the magnetic particles, but should be combined with rock-magnetic measurements which provide the magnetic characteristics of the bulk grain.

Separation of single crystals for paleomagnetic measurements

Oriented samples of single crystals can be obtained by isolating the target crystal in a thin section cut from a rock sample (e.g., Geismann et al. 1988; Cottrell and Tarduno 2000; Tarduno et al. 2007; 2020; Bono and Tarduno 2015). Thin sections thicker than usual (for example, >1 mm, depending on the grain size) are made for this purpose. Before slicing the sample, a fiducial notch for the orientation should be cut in the side of the sample, and orientation grids should be scribed on the surface after slicing. Portions in the thin section other than the desired single crystal are mechanically trimmed off, or abraded away using alumina or other etching powder. Finally, the section is cut into smaller subsections that consist of a single crystal. Sonication at each step and rinsing by hydrochloric acid (HCl) is effective in preventing contamination. During this process, samples may experience heating up to about 100 °C. Tungsten, diamond, or brass wire saws are used in cutting out the ‘thick’ thin sections and subsampling from them (e.g., Fu et al. 2014; 2020; Bryson et al. 2020a). Non-magnetic Dremel type hand tools (e.g., Bezaeva et al. 2014; Font et al. 2014) may also be used.

Unoriented single crystal samples are obtained by crushing rock samples using non-magnetic tools. Large grains of feldspars, quartz and pyroxenes may be selected by eyes, and sorting by sieves with appropriate mesh opening help getting specific minerals, such as zircon, with a certain grain size. To concentrate zircons, aqueous panning technique and heavy liquid separation are effective (e.g., Sato et al. 2015a; Kato et al. 2018; Fu et al. 2017; Tarduno et al. 2023). Care must be taken to ensure the heavy liquids are pure; the materials should not be reused for each separation to avoid contamination. For any silicate mineral, grains with no visible cracks or large opaque inclusions should be selected (e.g., Tarduno et al. 2006; 2015) under the binocular stereo microscope using non-magnetic tweezers. Sonication and/or rinsing by HCl are adopted to remove invisible surface magnetic contamination. This method is suitable when using samples with relatively small particle sizes, which are difficult to cut out, or when a large number of samples are needed to be processed.

Instruments for remanence measurements and paleointensity experiments

Three-component DC superconducting quantum interference device (SQUID) magnetometers, scanning

SQUID microscope (SSM), and quantum diamond microscope (QDM) are employed for SCP and related studies.

An ultrasensitive 3-component DC SQUID magnetometer with a sample hole of 6.3 mm in diameter (2G Enterprises) is used for the SCP studied in Tarduno et al. (2010; 2012; 2015; 2020; 2021; 2023). This magnetometer has a sensitivity one order of magnitude higher than that of SQUID magnetometers with a 42 mm bore hole (2G Enterprises Model 755). Tarduno et al. (2015) mounted their zircon samples (>150 μm) at the end of 0.5 mm fused quartz square tubes, and set them on the end of a quartz rod of 2.0 mm in diameter for translation into the measurement space of the SQUID magnetometer. The magnetization of these tubes and rods was $<1 \times 10^{-13} \text{ Am}^2$.

Conventional DC SQUID magnetometers (2G Enterprises Model 755 or 760) are also used in many studies (e.g., Cottrell and Tarduno 1999; Tarduno et al. 2007; Usui and Nakamura 2009; Sato et al. 2015a; Kato et al. 2018; Bono et al. 2019a, b). In Kato et al. (2018), single crystal sample of zircon, quartz and plagioclase was embedded in a pit 1.0 mm in diameter drilled to a 7.0 mm square non-alkali glass plate (Eagle XG, Corning, 1.1 mm thick) and secured by stuffing fine grained high purity SiO_2 powder to the pit (Fig. 4). Upon remanence measurements, the glass plate was attached to a rod made by Acrylonitrile butadiene styrene (ABS; 7.0 mm in diameter and 60 mm in length), which was fixed to the discrete sample handling system of the DC SQUID magnetometer (Sato et al. 2015a). The magnetization of the glass plate and SiO_2 powder after subtracting that of the ABS rod was below the practical detection limit of the magnetometer of $4 \times 10^{-12} \text{ Am}^2$ (Sato et al. 2015a; Kato et al. 2018).

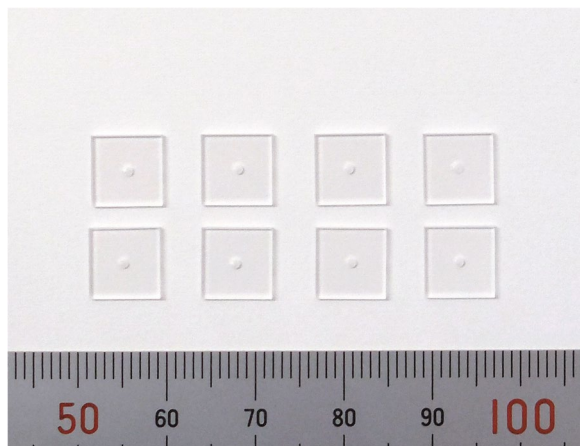


Fig. 4 Glass plate holders for single crystal measurements

The SSM is also employed for paleointensity experiments (Weiss et al. 2007; Lima and Weiss 2016; Fu et al. 2014; 2017; Tarduno et al. 2020; Borlina et al. 2021). Magnetic moment of single crystals can be estimated by inversion of magnetic field maps (e.g., Lima et al. 2013) or fitting the scanned distribution of the magnetic field component orthogonal to the sample surface by that calculated for a dipole moment (Lima and Weiss 2016). Ideally, the sensitivity of SSM reaches $\sim 10^{-15} \text{ Am}^2$ by making the distance between the sensor and the sample as close as possible ($\sim 200 \mu\text{m}$), but practically there are sources of noise and such extra-high sensitivity is hardly achieved. For SCP measurements using SSM, the single crystal samples are embedded in pits drilled into a magnetically clean and heat resistant glass slide so that a dozen samples can be scanned at once in a fixed orientation throughout the experimental process (Fu et al. 2017).

The QDM has extra high spatial resolution up to 1.17 μm (Borlina et al. 2021), and is used to map the magnetization distribution within single silicate samples to make inferences on the origins of magnetic inclusions and measure the magnetization of very small areas (e.g., Fu et al. 2014; 2017; 2020; 2021; Tang et al. 2019; Borlina et al. 2020; 2021). A major difference with the SQUID is that the QDM measurements need to be conducted under the presence of a bias field of $\sim 10 \mu\text{T}$ (Glenn et al. 2017). To isolate the remanent magnetization, the measurements are conducted with antiparallel bias fields and the field maps are summed to cancel out the contribution of induced magnetization (e.g., Fu et al. 2014). However, this approach is incomplete if there is magnetic anisotropy. Moreover, the QDM is most sensitive to 1 μm in depth from the surface of the sample, which may not sample a sufficient volume/number of magnetic particles to yield meaningful paleomagnetic information (Berndt et al. 2016; Tarduno et al. 2020). Paleomagnetic measurements using the QDM and their interpretation should be done carefully taking these advantages and limitations into account.

For thermal demagnetization and the heating procedures in paleointensity experiments, CO_2 laser (e.g., Tarduno et al. 2007) and infrared heating (Usui et al. 2015) have been used besides conventional paleomagnetic ovens. The small size of the single crystals enables usage of these alternative techniques, which minimize thermal alteration during laboratory processes by shortening the heating times by orders of magnitude compared to conventional methods.

Paleointensity protocols and selection criteria for successful results

SCP studies are conducted employing the variations of the Thellier-Thellier method (e.g., Thellier and Thellier

1959; Coe 1967; Riisager and Riisager 2001; Yu and Dunlop 2003; Tauxe and Staudigel 2004; Yu et al. 2004). The Thellier–Coe method (Thellier and Thellier 1959; Coe 1967) which incorporates partial TRM checks to assess alteration is most frequently applied (e.g., Cottrell and Tarduno 1999; 2000; Tarduno et al. 2001; 2002; 2007; 2010; 2012; 2015; 2020; 2021; 2023; Smirnov et al. 2003; Tarduno and Cottrell 2005; Cottrell et al. 2008; Usui and Nakamura 2009; Bono et al. 2019a; Zhou et al. 2022). The IZZI protocol of the Thellier–Coe method (Tauxe and Staudigel 2004; Yu et al. 2004) is also used (Fu et al. 2017; Usui and Tian 2017; Borlina et al. 2022). Selection criteria for reliable paleointensity estimate are set (e.g., Cottrell and Tarduno 2000), generally following those for whole-rock samples but sometimes relaxed reflecting the nature of the samples, such as the very weak magnetization. Bono et al. (2019a) and Zhou et al. (2022) used multiple categories with different numbers of criteria met. The studies on Archean to Hadean detrital zircons also employ determinations at a single step at 565 °C (Tarduno et al. 2015; 2020; 2023). This method is more suited for field presence/absence or order-of-magnitude estimates, but is less measurement/time intensive and yields more data.

Kato et al. (2018) applied the Tsunakawa–Shaw method (Tsunakawa and Shaw 1994; Yamamoto et al. 2003; 2015; Mochizuki et al. 2004; Oishi et al. 2005) on SCP study of plagioclase with exsolved magnetite. This method employs low-temperature demagnetization (LTD) to selectively demagnetize the coarse-grained magnetite (e.g., Ozima et al. 1964; Heider et al. 1992), stepwise alternating field demagnetization (AFD), twice full-TRM impartment, and correction for possible laboratory-heating alternation and/or anisotropy using anhysteretic remanent magnetization (ARM) which is checked by replicating the procedure. The main advantages of this method are: (i) thermal alteration is minimized by heating the sample to a temperature above the Curie point only twice, (ii) the influence of non-ideal coarse grains is avoided by LTD and AFD. For the SCP study, selection criteria which were slightly relaxed from those set for whole-rock volcanic samples (Yamamoto and Tsunakawa 2005) were adopted.

Treatment of magnetic anisotropy

Some single crystals containing exsolved magnetite exhibit large magnetic anisotropy (Feinberg et al. 2006; Usui and Nakamura 2009; Usui et al. 2015), whereas others show moderate or minor net anisotropy (Kato et al. 2018; Bono et al. 2019a; Zhou et al. 2022). In the case of samples with strong anisotropy, the direction of the remanence deviates from that of the external field and the efficiency of remanence acquisition differs by the

direction of the external field against the anisotropy axes of the sample. Thus, to precisely reconstruct the paleomagnetic information, treatment for anisotropy correction is essential (Tarduno et al. 2006).

To estimate the degree of anisotropy and correct for the possible bias on paleointensity estimates, anisotropy tensors of TRM can be determined by least-square fitting the remanences acquired along different axes (Hext 1963). For plagioclase crystals with large anisotropy, Usui et al. (2015) demonstrated that the bias caused by anisotropy can be mitigated by taking the geometric mean of paleointensity data from a few tens of grains. Kato et al. (2018) estimated the anisotropy of ARM of single plagioclase crystals and concluded that for their samples the bias from anisotropy are likely canceled by averaging the paleointensity results from the nine successful samples. They found that the degree of anisotropy gets larger at higher coercivity, suggesting that the acicular magnetite grains are responsible for the high coercivity component. During the Thellier–Coe paleointensity experiments, Bono et al. (2019a) and Zhou et al. (2022) calculated the anisotropy correction factor (Veitch et al. 1984) after the NRM begins to unblock by measuring the TRM acquired by field applied by orthogonal directions.

In samples dominantly containing exsolved magnetite, the relationship between the intensity of TRM and the applied field may be hyperbolic tangential, not proportional as assumed in standard paleointensity protocols (Néel 1949; Selkin et al. 2007). Usui and Nakamura (2009) measured the TRM obtained at different applied fields and demonstrated that correction for hyperbolic tangential TRM acquisition is effective to yield precise paleointensity estimates. They also attempted to make corrections for both magnetic anisotropy and nonlinear TRM acquisition simultaneously, but found that the error gets too large mainly due to the difficulty of precise determination of the anisotropy tensor. Nonlinearity in TRM acquisition efficiency due to the strong anisotropy can be evaluated by checking the consistency of paleomagnetic estimates based on different applied fields (Bono et al. 2019a; Zhou et al. 2022).

Assessment and correction for cooling rate effect

To determine the average paleointensity using intrusive rocks, it is sometimes necessary to compensate for the difference in TRM acquisition efficiency due to the difference in cooling rates when the NRM was acquired and in the laboratory. The effect of cooling rate on the TRM acquisition differs by the domain state. SD grains acquire larger TRM when cooled slower (Halgedahl et al. 1980) and vice versa for MD grains (Yu 2011). PSD grains are the intermediate of SD and MD grains and thus the influence from cooling rate is insignificant (Yu 2011). In

the case of SCP studies using intrusive rocks, the effect of cooling rate is assessed by calculating the cooling time of the pluton body by a thermal diffusion model or radiometric dating by different closure temperature, and estimating the magnetic grain size distribution by rock magnetic measurements (e.g., Tarduno et al. 2015; Kato et al. 2018).

Overview of paleointensity and related studies using single crystals or single constituents published after 2006

Improvements in sample handling and rock magnetic characterizations described above have extended the applications of single silicate paleomagnetism, and significant progresses have been made in areas highlighted as future studies by Tarduno et al. (2006). Utilization of detrital zircon enables retrieval of magnetic information from Hadean and Eoarchean samples (Tarduno et al. 2015; 2020; 2023). Intrusive rocks which were less used in paleomagnetic studies have become the major targets in SCP studies, and the number of reliable estimates on time-averaged paleointensity is increasing (Tarduno et al. 2007; 2010; Kato et al. 2018; Bono et al. 2019a; Zhou et al. 2022). Even for volcanic rocks which have been the main objectives in conventional whole-rock studies, separating appropriate silicate crystals provides a chance to conduct paleointensity studies on more suitable targets (Cottrell et al. 2008; Usui and Tian 2017). Moreover, histories of the magnetic field of other solar system bodies and the paleo field of the solar nebula have been investigated by measurements on minerals and constituents separated from various extraterrestrial materials (Tarduno et al. 2012; 2021; Fu et al. 2014; 2020; Borlina et al. 2021). In this section, we briefly overview the SCP and related studies on terrestrial and extraterrestrial samples published after Tarduno et al. (2006).

Terrestrial samples

Presence of a geomagnetic field requires core heat flux larger than that can be maintained by thermal conduction. Therefore, determining how long the Earth's magnetic field has existed is important for understanding the thermal history of the Earth. Tarduno et al. (2015; 2020) reported relatively high paleointensity (3.6–29.4 μT) from 4.2 to 3.3 Ga Jack Hills zircons, supporting that the geomagnetic field and associated shielding from the solar wind date back to the Hadean. Tarduno et al. (2023) reported paleointensity from 3.9 to 3.3 Ga zircons from the Barberton Greenstone Belt, South Africa. On the basis of the nearly constant paleointensity values for the Barberton Greenstone Belt and the Jack Hills samples between about 3.9 to 3.4 Ga, they argued the stagnant-lid tectonics without plate motions during the period.

SCP studies on detrital zircons require the following procedure with selection criteria set on each step; screening of grains which may yield robust paleointensity (size, starting NRM, surface condition, etc.), paleointensity experiments, and U–Pb age determinations with care on metamictization and zoning. Unfortunately, age determinations must be carried out after paleointensity experiments to avoid alteration, putting the low-success and labor-intensive procedure first. This naturally produces a strong filter on experimental success rate; even more so if the study goals include defining a robust dipole moment estimate for a specific time interval.

Determination of whether the pre-depositional magnetization is preserved is critical, especially for Archean to Hadean detrital grains with complex metamorphic and deformation history. Here we summarize field tests at multiple levels and examination by other methods. Positive conglomerate tests at cobble-scale are reported for the Jack Hills (Tarduno and Cottrell 2013; Bono et al. 2018) and the Barberton Greenstone Belt (Usui et al. 2009). Characterization of diverse magnetic inclusions including PSD/SD magnetite with high unblocking temperature in the zircon-bearing Jack Hills quartzite are revealed by Dare et al. (2016) and Bono et al. (2019b), supporting the validity of the conglomerate tests. Microconglomerate test on the Jack Hills zircons was positive and negative for high and low unblocking temperature component, respectively, suggesting the high component survived metamorphic reheating while the low component was remagnetized (Tarduno et al. 2015; 2020). Microscopic distribution of Pb (Tarduno et al. 2015) and Li zoning (Tarduno et al. 2020) within zircon grains also indicate that those grains have not been heated above 475 °C, which is similar to the post-depositional peak metamorphic conditions of greenschist facies (Rasmussen et al. 2010). Furthermore, an inverse microconglomerate test on fuchsite (Cottrell et al. 2016) and a cluster analysis of paleomagnetic directions from quartzite clasts (Bono et al. 2018) put constraints on the temperature and timing of peak metamorphism, supporting that the zircons retain remanence older than the depositional age of the Jack Hills conglomerate (ca. 2.65–3.05 Ga; Rasmussen et al. 2010). In opposition to these studies, Weiss et al. (2015) questioned the preservation of pre-depositional magnetization in the Jack Hills zircons based on multiple field tests, rock-magnetic surveys and SEM analysis on various rocks from the nearby sites and argued that they were possibly remagnetized probably after ca. 2.65 Ga, suggesting regional heterogeneity. A comment by Bono et al. (2016) pointed out that the post 2.65 Ga direction claimed by Weiss et al. (2015) was not present in their raw microconglomerate data and was instead due to the inappropriate use of statistics. Furthermore,

magnetizations with unblocking temperatures above the peak metamorphic temperature were not isolated in Weiss et al. (2015), and information of the magnetization that predates the metamorphic reheating at ca. 2.65 Ga cannot be obtained (Dare et al. 2016).

Whether the paleointensity from detrital zircons are truly from the ages of the grains may be tested by the age versus paleointensity data themselves by the following logics. First, if the timing of magnetization acquisition differs from the U–Pb age of the grain, there should be no distinctive trend in paleointensity versus time diagram. Instead, one can see a trend in the reported results; relatively high values in the Hadean, low Eoarchean–Paleoarchean values, and increasing values in the late Paleoarchean (Tarduno et al. 2015; 2020; 2023). Second, if the reconstructed time variation of paleointensity reflects the history of the main field, it should be a global signature also seen in other cratons. The records from the Jack hills and the Barberton Greenstone Belt agree with each other, passing this test (Tarduno et al. 2015; 2020; 2023). Nevertheless, paleointensity estimates from this time window are still sparse, especially for those with multiple temperature steps on paleointensity determination, and data from different geological units and different research groups should be added in the future.

Long-term changes of the geomagnetic field should be reflecting the evolution of the overlying mantle and the inner core, which are the upper and lower boundaries that govern the convection in the liquid core. Correlation between paleomagnetic variations and mantle activity has been pointed out in a number of studies (e.g., McFadden and Merrill 1984; Tarduno et al. 2006; Courtillot and Olson 2007; Tarduno 2009; Biggin et al. 2012), which can be explained by that the behavior of the geomagnetic field is influenced by the total amount and spatial pattern of the heat flux from the core to the mantle, suggested by numerical dynamo simulations (e.g., Glatzmaier et al. 1999; Takahashi et al. 2008; Olson et al. 2010; Amit et al. 2015). Crystallization of the solid inner core accompanied with chemically driven convection has increased the power of the geodynamo, and possibly caused an observable shift in the behavior of the geomagnetic field (e.g., Stevenson et al. 1983; Aubert et al. 2010; Labrosse 2015). Note that the potential for detecting inner core growth through field strength alone has been questioned (e.g., Landeau et al. 2017), but is broadly supported by thermal evolution geodynamo models (e.g., Davies et al. 2022).

Several studies use slowly cooled intrusive rocks instead of volcanic rocks in the hope of averaging out secular variations. Quartz and microcline crystals separated from 3.2 Ga granitic plutons in the Kaapvaal craton show virtual dipole moment of $6.4\text{--}7.5 \times 10^{22} \text{ Am}^2$ before cooling rate corrections (Tarduno et al. 2007). Similar

intensities for ~ 3.45 Ga were also obtained using quartz crystals in shallow intrusive rocks (Tarduno et al. 2010), although this record may average only tens to hundreds of years of secular variations. These two intrusive records are currently regarded as the most reliable paleointensity values for Archean, corroborated by rock-magnetic evaluations.

Earlier efforts to use single silicate with exsolved magnetite for paleointensity found very strong remanence anisotropy as a main challenge (Feinberg et al. 2006; Usui and Nakamura 2009; Usui et al. 2015). Nevertheless, more recent studies revealed that in some case plagioclase crystals with exsolved magnetite only has moderate net anisotropy, and reasonable average paleointensity estimates have been reported with or without anisotropy corrections (Kato et al. 2018; Bono et al. 2019a; Zhou et al. 2022). Most probably the magnetic anisotropy degree depends on lithology, but systematic investigation on this issue has not been conducted. Plagioclase crystals with exsolved magnetite have been used to define paleointensity during the Ediacaran (Bono et al. 2019a) and the early Cambrian (Zhou et al. 2022) periods. Bono and Tarduno (2015) reported near antipodal directions in oriented single feldspar crystals in sub centimeter scale indicating a very high reversal rate in the Ediacaran period. Together with whole-rock paleointensity data from two continents (Shcherbakova et al. 2020; Thallner et al. 2021a, b; 2022), these records suggest that the dipole was extremely low and frequently reversing at around 565 Ma, followed by a rather rapid recovery by ~ 532 Ma. This geodynamo behavior is interpreted as a sign of inner core nucleation and growth (Bono et al. 2019a; Shcherbakova et al. 2020).

Only a rather small number of SCP data has been reported since 2006 from volcanic rocks; however, this approach should gather more attention. Cottrell et al. (2008) studied basaltic lava flows near the end of the Permo–Carboniferous Superchron. While it is indicated that paleointensity was higher than the present-day field, the number of data was insufficient to average out secular variations. Usui and Tian (2017) also reported paleointensity from lavas within the Permo–Carboniferous Superchron. Their directional data indicate that the lava sequence does not average out secular variation, either. One of the original motivations to introduce SCP was to circumvent the potential bias of low paleointensity before 10 Ma records (Tarduno and Smirnov 2004; Tarduno et al. 2006), which may be due to low-temperature oxidation. These authors pointed out that many whole rock data are comparable to the paleointensity during geomagnetic reversals or excursions. Analyses of an updated database with more stringent criteria (Bono et al. 2022) do not completely eliminate this problem, highlighting

the needs for larger scale comparisons of SCP and whole rock data obtained using modern measurement protocols.

Single crystal magnetic measurements have also inspired applications other than paleointensity. Nearly single-domain exsolved magnetite provides important test cases to connect magnetic measurements to mineralogical observations (Nikolaisen et al. 2022). In particular, relatively high abundance of exsolved magnetite within plagioclase and pyroxenes have enabled direct determination of 3D morphologies of magnetite crystals. These morphologies are in turn fed into micromagnetic simulations, providing predictions of magnetic properties that can directly be compared with single crystal measurements. At present, it is still difficult to measure all grains within single crystals of sufficient size to be measured by magnetometers, and some extrapolation is necessary. Future effort should fill the gap between single silicate measurements and single magnetic mineral characterization. Another application is environmental magnetism using sediments (Hounslow and Morton 2004; Chang et al. 2016; Usui et al. 2018). Magnetic inclusions in silicate are expected to reflect source rock composition better than the whole sediment properties, which might be affected by post-depositional diagenesis.

Extraterrestrial samples

Paleointensity experiments using single crystal or single constituent techniques have also been applied for extraterrestrial samples. The paleointensity studies for extraterrestrial samples can be classified into two groups: the silicate crystals separated from host rocks (Tarduno et al. 2012, 2021) and the chondrules extracted from chondrite samples (Fu et al. 2014; 2020; Borlina et al. 2021).

The origin of pallasite meteorites that are mainly composed of olivine crystal and FeNi metal have been questioned since their discovery. To answer this question, Tarduno et al. (2012) conducted Thellier-Coe paleointensity experiments for single olivine crystals separated from the Imilac and Esquel main group pallasites. They selected the olivine crystals lacking visible inclusions, which likely contain small FeNi inclusions and show the PSD to SD hysteresis behaviors. The paleointensity values are successfully obtained as $122.3 \pm 14.4 \mu\text{T}$ (Esquel) and $73.6 \pm 8.1 \mu\text{T}$ (Imilac). Similar paleointensity estimates are also reported by Bryson et al. (2015), based on high-resolution nanomagnetic imaging by X-ray magnetic circular dichroism (Stöhr 1999; van der Laan 2013) and simulation on magnetic nanostructures magnetized by variable field components. On the basis of the paleointensity values of two different pallasites and thermal modelings of the parent protoplanet, the pallasite meteorites are suggested to be formed when liquid FeNi from the core of an

impactor was injected as dikes into the shallow mantle of a ~ 200 -km-radius protoplanet. This model is further supported by Windmill et al. (2022), who studied the oxygen isotopic disequilibrium between olivine and chromite in the pallasites.

Whether the Moon had a long-lived magnetic field provides essential information about the evolution of its interior and surface. The bulk lunar magnetic samples typically contain large MD grains and often show non-ideal MD-like magnetic characteristics, and thus, the SCP technique plays an important role to overcome such difficulties in paleointensity measurements. Tarduno et al. (2021) conducted TRM-based paleointensity experiments for plagioclase and/or pyroxene crystals separated from the lunar basalt samples with ages of 3.2–3.9 Ga collected in the Apollo 12, 14, and 17 missions. The silicate samples contain small native iron particles with sub-micrometer grain size, of which the magnetic domain states are predicted to be in the SD or single vortex (SV). The NRM intensities of silicate crystals were very weak ($1.2\text{--}3.9 \times 10^{-12} \text{ Am}^2$) and did not show consistent directions after thermal demagnetization at 590 °C, agreeing with a null magnetization. TRM acquisition experiments with alteration checks were performed, and it was demonstrated that these crystals can record a field with an efficiency near 100% if it had been present on the Moon. Instead, the data point to null ambient magnetization values. Null lunar field agrees with a previous study also based on thermal methods (Lawrence et al. 2008) but contradicts with high ($\sim 100 \mu\text{T}$) fields reported for overlapping ages implying a long-lived lunar dynamo (e.g., Cournède et al. 2012). Note that the latter is obtained by nonthermal methods, for which great concerns on reliability have been raised (Dunlop and Özdemir 1997; Lawrence et al. 2008).

The magnetic field in the solar nebula was coupled to the gas, and had a significant influence on the formation of the solar system. The reconstruction of nebular field history is a critical issue in planetary science. Paleofield records of the solar nebula have been studied using the whole rock measurements of carbonaceous chondrites and returned samples from the asteroid Ryugu. However, these records were attributed to the chemical remanent magnetization (CRM) during aqueous alterations in parent bodies (Borlina et al. 2022; Bryson et al. 2020a; Cournède et al. 2015; Fu et al. 2021; Gattacceca et al. 2016; Sato et al. 2022) and the TRM in a parent body (Bryson et al. 2020b). Therefore, paleointensity experiments using separated chondrules play an important role in reconstructing the paleo field before parent body formations. Fu et al. (2014) separated the dusty olivine bearing chondrules from the Semarkona ordinary chondrite, and measured the ARM-based paleointensity. The

dusty olivine crystals contain nearly pure kamacite with submicrometer sizes, which likely have SD or SV states. The paleointensity values at 2.0 ± 0.8 million years after the calcium–aluminum-rich inclusion (CAI) formation are estimated to be $27 \pm 8 \mu\text{T}$. Borlina et al. (2021) also conducted paleointensity experiments for dusty olivine bearing chondrules in the DOM 08006 and ALHA77307 Ornans type (CO) carbonaceous chondrites. The dusty olivines contain fine-grained kamacite crystals. The paleointensity values at 2.2 ± 0.8 Ma after the CAI formation are obtained from the ARM normalization method as $30 \pm 10 \mu\text{T}$ (DOM 08006) and $59 \pm 31 \mu\text{T}$ (ALHA77307). For the Renazzo type (CR) carbonaceous chondrites, Fu et al. (2020) extracted 7 subsamples from an iron sulfide-rich chondrule rims in GRA 95229 and 11 subsamples from four chondrules in LAP 02342, in which FeNi and Fe sulfides are the main ferromagnetic phases. The maximum paleofield values at $3.7^{+0.3}_{-0.2}$ Myr after CAI formation were evaluated on the basis of ARM acquisition abilities as $8.1 \pm 5.4 \mu\text{T}$ (GRA 95229) and $4.0 \pm 2.2 \mu\text{T}$ (LAP 02342). Meanwhile, there is considerable evidence that FeNi magnetic minerals can have unusual magnetic behavior including intrinsic magnetizations that may mimic the signals of an ancient field (e.g., Brecher and Albright 1977). O'Brien et al. (2020) demonstrated that such an effect can be detected by thermal analyses, while non-thermal paleointensity estimates may not reflect the ancient field. For the reconstruction of the nebular field, the single-constituent techniques have only been applied for chondrules. Similar study of other constituents such as CAIs will provide nebular field information temporally and spatially different from that of chondrules.

Conclusion

Nearly a quarter of a century has passed since the development of the SCP (Cottrell and Tarduno 1999), and significant progress has been made in research in areas predicted by early reviews (Tarduno et al. 2006; Tarduno 2009) as future challenges. SCP techniques have broad utility in paleointensity studies for the Earth, extraterrestrial bodies, and the solar nebular, especially in the case that the paleointensity measurements are difficult in whole rock samples. Zircon, quartz and plagioclase crystals with invisible magnetic xenocrysts are the most robust targets due to the high probability of the primary origin of magnetization. When studying these samples, a large number of crystals should be screened to find samples with sufficient magnetic inclusions and stable magnetization. Silicate crystals containing exsolved magnetite also have the potential to play a leading role in elucidating

long-period geomagnetic variations related to the evolution of the Earth's interior, although the effect of the large magnetic anisotropy should be considered upon measurements.

So far, only several groups of scientists are involved in SCP studies. Although measuring very weak magnetization requires highly sensitive equipment such as ultrasensitive small-bore SQUID magnetometer, SSM, or QDM, the remanence of single silicate crystals can be often measured using the conventional SQUID magnetometer. The future SCP experiments by various scientists in many laboratories will further advance the SCP method and will bring our understanding of past magnetic fields forward.

Abbreviations

AGM	Alternating gradient magnetometer
ARM	Anhyseretic remanent magnetization
CAI	Calcium–aluminum-rich inclusion
CRM	Chemical remanent magnetization
EDS	Energy dispersive X-ray spectroscopy
FC	Field cooling
FORC	First-order reversal curve
IRM	Isothermal remanent magnetization
LTD	Low-temperature demagnetization
MD	Multidomain
MPMS	Magnetic property measurement system
NRM	Natural remanent magnetization
PSD	Pseudo single domain
QDM	Quantum diamond microscope
SCP	Single silicate crystal paleointensity
SD	Single domain
SEM	Scanning electron microscope
SIRM	Saturation IRM
SQUID	Superconducting quantum interference device
SSM	Scanning SQUID microscope
SV	Single vortex
TCRM	Thermochemical remanent magnetization
TRM	Thermoremanent magnetization
ZFC	Zero-field cooling
ZFW	Zero-field warming

Acknowledgements

We thank two anonymous reviewers for their constructive comments. This study was performed under the cooperative research program of the Center for Advanced Marine Core Research, Kochi University (Accept Nos. 18A040, 18B037, 19A018, 19B016, 20A029, 20B026, 22A014, 22B013).

Author contributions

CK conceptualized the study. All authors contributed to discussion and writing the manuscript. All authors read and approved the final manuscript.

Funding

This study was supported by MEXT KAKENHI Grant Number JP23K13190 and JSPS KAKENHI Grant Number JP20J00400.

Availability of data and materials

Refer to the source articles.

Declarations

Ethics approval and consent to participate

Not applicable.

Consent for publication

Not applicable.

Competing interests

The authors declare no competing interests.

Author details

¹Faculty of Social and Cultural Studies, Kyushu University, Fukuoka, Japan. ²College of Science and Engineering, Kanazawa University, Kanazawa, Japan. ³Department of Earth and Planetary Science, The University of Tokyo, Tokyo, Japan. ⁴Institute of Space and Astronautical Science, Japan Aerospace Exploration Agency, Sagami-hara, Japan.

Received: 29 September 2023 Accepted: 8 March 2024

Published online: 29 March 2024

References

- Ageeva O, Habler G, Pertsev A, Abart R (2017) Fe-Ti oxide microinclusions in clinopyroxene of oceanic gabbro: Phase content, orientation relations and petrogenetic implication. *Lithos* 290–291:104–115. <https://doi.org/10.1016/j.lithos.2017.08.007>
- Ageeva O, Bian G, Habler G, Pertsev A, Abart R (2020) Crystallographic and shape orientations of magnetite micro-inclusions in plagioclase. *Contrib Mineral Petrol* 175:1–16. <https://doi.org/10.1007/s00410-020-01735-8>
- Amit H, Deschamps F, Choblet G (2015) Numerical dynamos with outer boundary heat flux inferred from probabilistic tomography—consequences for latitudinal distribution of magnetic flux. *Geophys J Int* 203:840–855. <https://doi.org/10.1093/gji/ggv332>
- Aubert J, Tarduno JA, Johnson CL (2010) Observations and models of the long-term evolution of Earth's magnetic field. *Space Sci Rev* 155:337–370. <https://doi.org/10.1007/s11214-010-9684-5>
- Behrens H, Johannes W, Schmalzried H (1990) On the mechanisms of cation diffusion processes in ternary feldspars. *Phys Chem Mineral* 17:62–78. <https://doi.org/10.1007/BF00209227>
- Berndt T, Muxworthy AR, Fabian K (2016) Does size matter? Statistical limits of paleomagnetic field reconstruction from small rock specimens. *J Geophys Res Solid Earth* 121(1):15–26. <https://doi.org/10.1002/2015JB012441>
- Besnus MJ, Meyer AJP (1964) Nouvelles données expérimentales sur le magnétisme de la pyrrhotine naturelle. In: *Proceedings of the international conference on magnetism: Nottingham, September, 1964*, The Physical Society, London, p 507–511
- Bezaeva NS, Badyukov DD, Nazarov MA, Rochette P, Feinberg JM, Markov GP, Borschneck D, Demory F, Gattacceca J, Borisovskiy SE, Skripnik AY (2014) Magnetic properties of the LL5 ordinary chondrite Chelyabinsk (fall of February 15, 2013). *Meteorit Planet Sci* 49:958–977. <https://doi.org/10.1111/maps.12307>
- Bian G, Ageeva O, Rečnik A, Habler G, Abart R (2021) Formation pathways of oriented magnetite micro-inclusions in plagioclase from oceanic gabbro. *Contrib Mineral Petrol* 176:104. <https://doi.org/10.1007/s00410-021-01864-8>
- Biggin AJ, Steinberger B, Aubert J, Suttie N, Holme R, Torsvik TH, van der Meer DG, van Hinsbergen DJJ (2012) Possible links between long-term geomagnetic variations and whole-mantle convection processes. *Nat Geosci* 5(8):526–533. <https://doi.org/10.1038/ngeo1521>
- Bogue SW, Gromme S, Hillhouse JW (1995) Paleomagnetism, magnetic anisotropy, and mid-Cretaceous paleolatitude of the Duke Island (Alaska) ultramafic complex. *Tectonics* 14(5):1133–1152. <https://doi.org/10.1029/95TC01579>
- Bono RK, Tarduno JA (2015) A stable Ediacaran Earth recorded by single silicate crystals of the ca 565 Ma Sept-Îles intrusion. *Geology* 43(2):131–134. <https://doi.org/10.1130/G36247.1>
- Bono RK, Tarduno JA, Cottrell RD (2016) Comment on: Pervasive remagnetization of detrital zircon host rocks in the Jack Hills, Western Australia and implications for records of the early dynamo, by Weiss et al. (2015). *Earth Planet Sci Lett* 450:406–408. <https://doi.org/10.1016/j.epsl.2016.06.006>
- Bono RK, Tarduno JA, Dare MS, Mitra G, Cottrell RD (2018) Cluster analysis on a sphere: Application to magnetizations from metasediments of the Jack Hills, Western Australia. *Earth Planet Sci Lett* 484:67–80. <https://doi.org/10.1016/j.epsl.2017.12.007>
- Bono RK, Tarduno JA, Nimmo F, Cottrell RD (2019a) Young inner core inferred from Ediacaran ultra-low geomagnetic field intensity. *Nat Geosci* 12:143–147. <https://doi.org/10.1038/s41561-018-0288-0>
- Bono RK, Tarduno JA, Cottrell RD (2019b) Primary pseudo-single and single-domain magnetite inclusions in quartzite cobbles of the Jack Hills (Western Australia): implications for the Hadean geodynamo. *Geophys J Int* 216:598–608. <https://doi.org/10.1093/gji/ggy446>
- Bono RK, Paterson GA, van der Boon A, Engbers YA, Grappone JM, Handford B, Hawkins LMA, Lloyd SJ, Sprain CJ, Thallner D, Biggin AJ (2022) The PINT database: a definitive compilation of absolute palaeomagnetic intensity determinations since 4 billion years ago. *Geophys J Int* 229(1):522–545. <https://doi.org/10.1093/gji/ggab490>
- Borlina CS, Weiss BP, Lima EA, Tang F, Taylor RJM, Einsle JF, Harrison RJ, Fu RR, Bell EA, Alexander EW, Kirkpatrick HM, Wielicki MM, Harrison TM, Ramezani J, Maloof AC (2020) Reevaluating the evidence for a Hadean-Eoarchean dynamo. *Sci Adv* 6:eaa9634. <https://doi.org/10.1126/sciadv.aav9634>
- Borlina CS, Weiss BP, Bryson JFJ, Bai XN, Lima EA, Chatterjee N, Mansbach EN (2021) Paleomagnetic evidence for a disk substructure in the early solar system. *Sci Adv* 7(42):eabj6928. <https://doi.org/10.1126/sciadv.abj6928>
- Borlina CS, Weiss BP, Bryson JFJ, Armitage PJ (2022) Lifetime of the outer solar system nebula from carbonaceous chondrites. *J Geophys Res Planets* 127(7):e2021JE007139. <https://doi.org/10.1029/2021JE007139>
- Brecher A, Albright L (1977) The thermoremanence hypothesis and the origin of magnetization in iron meteorites. *J Geomag Geoelec* 29:379–400. <https://doi.org/10.5636/jgg.29.379>
- Bryson JFJ, Nichols CIO, Herrero-Albillos J, Kronast F, Kasama T, Alimadadi H, van der Laan G, Nimmo F, Harrison RJ (2015) Long-lived magnetism from solidification-driven convection on the pallasite parent body. *Nature* 517:472–475. <https://doi.org/10.1038/nature14114>
- Bryson JFJ, Weiss BP, Lima EA, Gattacceca J, Cassata WS (2020a) Evidence for asteroid scattering and distal solar system solids from meteorite paleomagnetism. *Astrophys J* 892(2):126. <https://doi.org/10.3847/1538-4357/ab7cd4>
- Bryson JFJ, Weiss BP, Biersteker JB, King AJ, Russell SS (2020b) Constraints on the distances and timescales of solid migration in the early solar system from meteorite magnetism. *Astrophys J* 896:103. <https://doi.org/10.3847/1538-4357/ab91ab>
- Burton BP (1991) The interplay of chemical and magnetic ordering. In: Lindsley DH (ed) *Oxide minerals; petrologic and magnetic significance: reviews in mineralogy*, vol 25. De Gruyter, Berlin, pp 303–322
- Carter-Stiglitz B, Moskowitz B, Jackson M (2001) Unmixing magnetic assemblages and the magnetic behavior of bimodal mixtures. *J Geophys Res Solid Earth* 106(B11):26397–26411. <https://doi.org/10.1029/2001JB000417>
- Carter-Stiglitz B, Jackson M, Moskowitz B (2002) Low-temperature remanence in stable single domain magnetite. *Geophys Res Lett* 29:33–1–33–4. <https://doi.org/10.1029/2001GL014197>
- Chang L, Roberts AP, Heslop D, Hayashida A, Li J, Zhao X, Tian W, Huang Q (2016) Widespread occurrence of silicate-hosted magnetic mineral inclusions in marine sediments and their contribution to paleomagnetic recording. *J Geophys Res Solid Earth* 121:8415–8431. <https://doi.org/10.1002/2016JB013109>
- Coe RS (1967) Determination of paleo-intensities of the Earth's magnetic field with emphasis on mechanisms which could cause non-ideal behaviour in Thellier's method. *J Geomag Geoelectr* 19:157–179. <https://doi.org/10.5636/jgg.19.157>
- Cottrell RD, Tarduno JA (1999) Geomagnetic paleointensity derived from single plagioclase crystals. *Earth Planet Sci Lett* 169(1–2):1–5. [https://doi.org/10.1016/S0012-821X\(99\)0068-0](https://doi.org/10.1016/S0012-821X(99)0068-0)
- Cottrell RD, Tarduno JA (2000) In search of high-fidelity geomagnetic paleointensities: A comparison of single plagioclase crystal and whole rock Thellier-Thellier analyses. *J Geophys Res Solid Earth* 105(B10):23579–23594. <https://doi.org/10.1029/2000JB900219>
- Cottrell RD, Tarduno JA, Roberts J (2008) The Kiaman Reversed Polarity Superchron at Kiama: Toward a field strength estimate based on single

- silicate crystals. *Phys Earth Planet Inter* 169:49–58. <https://doi.org/10.1016/j.pepi.2008.07.041>
- Cottrell RD, Tarduno JA, Bono RK, Dare MS, Mitra G (2016) The inverse microconglomerate test: Further evidence for the preservation of Hadean magnetizations in metasediments of the Jack hills, Western Australia. *Geophys Res Lett* 43:4215–4220. <https://doi.org/10.1002/2016GL068150>
- Cournède C, Gattacceca J, Rochette P (2012) Magnetic study of large Apollo samples: Possible evidence for an ancient centered dipolar field on the Moon. *Earth Planet Sci Lett* 331–332:31–42. <https://doi.org/10.1016/j.epsl.2012.03.004>
- Cournède C, Gattacceca J, Gounelle M, Rochette P, Weiss BP, Zanda B (2015) An early solar system magnetic field recorded in CM chondrites. *Earth Planet Sci Lett* 410:62–74. <https://doi.org/10.1016/j.epsl.2014.11.019>
- Courtillot V, Olson P (2007) Mantle plumes link magnetic superchrons to Phanerozoic mass depletion events. *Earth Planet Sci Lett* 260(3):495–504. <https://doi.org/10.1016/j.epsl.2007.06.003>
- Dare MS, Tarduno JA, Bono RK, Cottrell RD, Beard JS, Kodama KP (2016) Detrital magnetite and chromite in Jack hills quartzite cobbles: Further evidence for the preservation of primary magnetizations and new insights into sediment provenance. *Earth Planet Sci Lett* 451:298–314. <https://doi.org/10.1016/j.epsl.2016.05.009>
- Davies CJ, Bono RK, Meduri DG, Aubert J, Greenwood S, Biggin AJ (2022) Dynamo constraints on the long-term evolution of Earth's magnetic field strength. *Geophys J Int* 228:316–336. <https://doi.org/10.1093/gji/ggab342>
- Davis KE (1981) Magnetite rods in plagioclase as the primary carrier of stable NRM in ocean floor gabbros. *Earth Planet Sci Lett* 55(1):190–198. [https://doi.org/10.1016/0012-821X\(81\)90098-4](https://doi.org/10.1016/0012-821X(81)90098-4)
- Dekkers MJ, Mattéi JL, Fillion G, Rochette P (1989) Grain-size dependence of the magnetic behavior of pyrrhotite during its low-temperature transition at 34 K. *Geophys Res Lett* 16:855–858. <https://doi.org/10.1029/GL016i008p00855>
- Dunlop DJ, Özdemir Ö (1997) *Rock magnetism—fundamentals and frontiers*. Cambridge University Press, Cambridge
- Feinberg JM, Wenk HR, Renne PR, Scott GR (2004) Epitaxial relationships of clinopyroxene-hosted magnetite determined using electron backscatter diffraction (EBSD) technique. *Am Miner* 89(2–3):462–466. <https://doi.org/10.2138/am-2004-2-328>
- Feinberg JM, Scott GR, Renne PR, Wenk HR (2005) Exsolved magnetite inclusions in silicates: Features determining their remanence behavior. *Geology* 33(6):513–516. <https://doi.org/10.1130/g21290.1>
- Feinberg JM, Harrison RJ, Kasama T, Dunin-Borkowski RE, Scott GR, Renne PR (2006) Effects of internal mineral structures on the magnetic remanence of silicate-hosted titanomagnetite inclusions: An electron holography study. *J Geophys Res Solid Earth* 111:B12S15. <https://doi.org/10.1029/2006JB004498>
- Fleet ME, Bilcox GA, Barnett RL (1980) Oriented magnetite inclusions in pyroxenes from the Grenville province. *Can Mineral* 18(1):89–99
- Font E, Veiga-Pires C, Pozo M, Carvallo C, de Siqueira Neto AC, Camps P, Fabre S, Mirão J (2014) Magnetic fingerprint of southern Portuguese speleothems and implications for paleomagnetism and environmental magnetism. *J Geophys Res Solid Earth* 119:7993–8020. <https://doi.org/10.1002/2014JB011381>
- Fu RR, Weiss BP, Lima EA, Harrison RJ, Bai XN, Desch SJ, Ebel DS, Suavet C, Wang H, Glenn D, Le Sage D, Kasama T, Walsworth RL, Kuan AT (2014) Solar nebula magnetic fields recorded in the Semarkona meteorite. *Science* 346(6213):1089–1092. <https://doi.org/10.1126/science.1258022>
- Fu RR, Weiss BP, Lima EA, Kehayias P, Araujo JFDF, Glenn DR, Gelb J, Einsle JF, Bauer AM, Harrison RJ, Ali GAH, Walsworth RL (2017) Evaluating the paleomagnetic potential of single zircon crystals using the Bishop Tuff. *Earth Planet Sci Lett* 458:1–13. <https://doi.org/10.1016/j.epsl.2016.09.038>
- Fu RR, Kehayias P, Weiss BP, Schrader DL, Bai XN, Simon JB (2020) Weak magnetic fields in the outer solar nebula recorded in CR chondrites. *J Geophys Res Planet* 125(5):e2019JE006260. <https://doi.org/10.1029/2019JE006260>
- Fu RR, Volk MWR, Bilardello D, Libourel G, Lesur GRJ, Ben Dor O (2021) The fine-scale magnetic history of the Allende meteorite: implications for the structure of the solar nebula. *AGU Adv* 2:e2021AV000486. <https://doi.org/10.1029/2021AV000486>
- Gattacceca J, Weiss BP, Gounelle M (2016) New constraints on the magnetic history of the CV parent body and the solar nebula from the Kaba meteorite. *Earth Planet Sci Lett* 455:166–175. <https://doi.org/10.1016/j.epsl.2016.09.008>
- Gee JS, Yu Y, Bowles J (2010) Paleointensity estimates from ignimbrites: An evaluation of the Bishop Tuff. *Geochem Geophys Geosyst* 11(3):Q03010. <https://doi.org/10.1029/2009GC002834>
- Geissman JW, Harlan SS, Brearley AJ (1988) The physical isolation and identification of carriers of geologically stable remanent magnetization: paleomagnetic and rock magnetic microanalysis and electron microscopy. *Geophys Res Lett* 15:479–482. <https://doi.org/10.1029/GL015i005p00479>
- Ghiorso MS (1997) Thermodynamic analysis of the effect of magnetic ordering on miscibility gaps in the FeTi cubic and rhombohedral oxide minerals and the FeTi oxide geothermometer. *Phys Chem Mineral* 25:28–38. <https://doi.org/10.1007/s002690050083>
- Glatzmaier GA, Coe RS, Hongre L, Roberts PH (1999) The role of the Earth's mantle in controlling the frequency of geomagnetic reversals. *Nature* 401(6756):885–890. <https://doi.org/10.1038/44776>
- Glenn DR, Fu RR, Kehayias P, Le Sage D, Lima EA, Weiss BP, Walsworth RL (2017) Micrometer-scale magnetic imaging of geological samples using a quantum diamond microscope. *Geochem Geophys Geosyst* 18:3254–3267. <https://doi.org/10.1002/2017GC006946>
- Halgedahl SL, Day R, Fuller M (1980) The effect of cooling rate on the intensity of weak-field TRM in single-domain magnetite. *J Geophys Res Solid Earth* 85:3690–3698. <https://doi.org/10.1029/JB085iB07p03690>
- Heider F, Dunlop DJ, Soffel HC (1992) Low-temperature and alternating field demagnetization of saturation remanence and thermoremanence in magnetite grains (0.037 μm to 5 mm). *J Geophys Res Solid Earth* 97:9371–9381. <https://doi.org/10.1029/91JB03097>
- Hext GR (1963) The estimation of second-order tensors, with related tests and designs. *Biometrika* 50(3–4):353–373. <https://doi.org/10.1093/biomet/50.3-4.353>
- Hounslow MW, Morton AC (2004) Evaluation of sediment provenance using magnetic mineral inclusions in clastic silicates: comparison with heavy mineral analysis. *Sediment Geol* 171:13–36. <https://doi.org/10.1016/j.sedgeo.2004.05.008>
- Kato C, Sato M, Yamamoto Y, Tsunakawa H, Kirschvink JL (2018) Paleomagnetic studies on single crystals separated from the middle Cretaceous Iritono granite. *Earth Planet Space* 70:176. <https://doi.org/10.1186/s40623-018-0945-y>
- Kosterov A (2003) Low-temperature magnetization and AC susceptibility of magnetite: effect of thermomagnetic history. *Geophys J Int* 154:58–71. <https://doi.org/10.1046/j.1365-246X.2003.01938.x>
- Labrosse S (2015) Thermal evolution of the core with a high thermal conductivity. *Phys Earth Planet Inter* 247:36–55. <https://doi.org/10.1016/j.pepi.2015.02.002>
- Landeau M, Aubert J, Olson P (2017) The signature of inner-core nucleation on the geodynamo. *Earth Planet Sci Lett* 465:193–204. <https://doi.org/10.1016/j.epsl.2017.02.004>
- Lawrence K, Johnson C, Tauxe L, Gee J (2008) Lunar paleointensity measurements: Implications for lunar magnetic evolution. *Phys Earth Planet Inter* 168:71–87. <https://doi.org/10.1016/j.pepi.2008.05.007>
- Lima EA, Weiss BP (2016) Ultra-high sensitivity moment magnetometry of geological samples using magnetic microscopy. *Geochem Geophys Geosyst* 17:3754–3774. <https://doi.org/10.1002/2016GC006487>
- Lima EA, Weiss BP, Baratchart L, Hardin DP, Saff EB (2013) Fast inversion of magnetic fields maps of unidirectional planar geological magnetization. *J Geophys Res Solid Earth* 118:2723–2752. <https://doi.org/10.1002/jgrb.50229>
- McFadden PL, Merrill RT (1984) Lower mantle convection and geomagnetism. *J Geophys Res Solid Earth* 89(B5):3354–3362. <https://doi.org/10.1029/JB089iB05p03354>
- Mochizuki N, Tsunakawa H, Oishi Y, Wakai S, Wakabayashi KI, Yamamoto Y (2004) Palaeointensity study of the Oshima 1986 lava in Japan: implications for the reliability of the Thellier and LTD-DHT Shaw methods. *Phys Earth Planet Inter* 146:395–416. <https://doi.org/10.1016/j.pepi.2004.02.007>
- Moskowitz BM, Frankel RB, Bazylinski DA (1993) Rock magnetic criteria for the detection of biogenic magnetite. *Earth Planet Sci Lett* 120:283–300. [https://doi.org/10.1016/0012-821X\(93\)90245-5](https://doi.org/10.1016/0012-821X(93)90245-5)

- Moskowitz BM, Jackson M, Kissel C (1998) Low-temperature magnetic behavior of titanomagnetites. *Earth Planet Sci Lett* 157:141–149. [https://doi.org/10.1016/S0012-821X\(98\)00033-8](https://doi.org/10.1016/S0012-821X(98)00033-8)
- Muxworthy AR, Evans ME (2012) Micromagnetics and magnetomineralogy of ultrafine magnetite inclusions in the Modipe Gabbro. *Geochem Geophys Geosyst* 14:921–928. <https://doi.org/10.1029/2012GC004445>
- Muxworthy AR, Evans ME, Scourfield SJ, King JG (2013) Paleointensity results from the late-Archaean Modipe Gabbro of Botswana. *Geochem Geophys Geosyst* 14(7):2198–2205. <https://doi.org/10.1002/ggge.20142>
- Nakada R, Sato M, Ushioda M, Tamura Y, Yamamoto S (2019) Variation of iron species in plagioclase crystals by X-ray absorption fine structure analysis. *Geochem Geophys Geosyst* 20(11):5319–5333. <https://doi.org/10.1029/2018GC008131>
- Néel L (1949) Théorie du trainage magnétique des ferro magnétiques en grains fins avec applications aux terres cuites. *Ann Geophys* 5:99–137
- Nikolaisen ES, Harrison R, Fabian K, Church N, McEnroe SA, Sørensen BE, Tegner C (2022) Hysteresis parameters and magnetic anisotropy of silicate-hosted magnetite exsolutions. *Geophys J Int* 229:1695–1717. <https://doi.org/10.1093/gji/ggac007>
- O'Brien T, Tarduno JA, Anand A, Smirnov AV, Blackman EG, Carroll-Nellenback J, Krot AN (2020) Arrival and magnetization of carbonaceous chondrites in the asteroid belt before 4562 million years ago. *Comm Earth Environ* 1:54. <https://doi.org/10.1038/s43247-020-00055-w>
- Oishi Y, Tsunakawa H, Mochizuki N, Yamamoto Y, Wakabayashi KI, Shibuya H (2005) Validity of the LTD-DHT Shaw and Thellier paleointensity methods: a case study of the Kilauea 1970 lava. *Phys Earth Planet Inter* 149:243–257. <https://doi.org/10.1016/j.pepi.2004.10.009>
- Olson P, Christensen UR (2006) Dipole moment scaling for convection-driven planetary dynamos. *Earth Planet Sci Lett* 250:561–571. <https://doi.org/10.1016/j.epsl.2006.08.008>
- Olson PL, Coe RS, Driscoll PE, Glatzmaier GA, Roberts PH (2010) Geodynamo reversal frequency and heterogeneous core–mantle boundary heat flow. *Phys Earth Planet Inter* 180(1–2):66–79. <https://doi.org/10.1016/j.pepi.2010.02.010>
- Özdemir Ö, Dunlop DJ, Moskowitz BM (1993) The effect of oxidation on the Verwey transition in magnetite. *Geophys Res Lett* 20:1671–1674. <https://doi.org/10.1029/93GL01483>
- Ozima M, Ozima M, Akimoto S (1964) Low temperature characteristics of remanent magnetization of magnetite—self-reversal and recovery phenomena of remanent magnetization. *J Geomag Geoelectr* 16:165–177. <https://doi.org/10.5636/jgg.16.165>
- Rasmussen B, Fletcher IR, Muhling JR, Wilde SA (2010) In situ U–Th–Pb geochronology of monazite and xenotime from the Jack Hills belt: Implications for the age of deposition and metamorphism of Hadean zircons. *Precam Res* 180:26–46. <https://doi.org/10.1016/j.precamres.2010.03.004>
- Riisager P, Riisager J (2001) Detecting multidomain magnetic grains in Thellier paleointensity experiments. *Phys Earth Planet Inter* 125:111–117. [https://doi.org/10.1016/S0031-9201\(01\)00236-9](https://doi.org/10.1016/S0031-9201(01)00236-9)
- Rochette P, Fillion G, Mattéi JL, Dekkers MJ (1990) Magnetic transition at 30–34 Kelvin in pyrrhotite: insight into a widespread occurrence of this mineral in rocks. *Earth Planet Sci Lett* 98:319–328. [https://doi.org/10.1016/0012-821X\(90\)90034-U](https://doi.org/10.1016/0012-821X(90)90034-U)
- Sato M, Yamamoto S, Yamamoto Y, Okada Y, Ohno M, Tsunakawa H, Maruyama S (2015a) Rock-magnetic properties of single zircon crystals sampled from the Tanzawa tonalitic pluton, central Japan. *Earth Planets Space* 67(1):150. <https://doi.org/10.1186/s40623-015-0317-9>
- Sato M, Yamamoto Y, Nishioka T, Kodama K, Mochizuki N, Usui Y, Tsunakawa H (2015b) Pressure effect on magnetic hysteresis parameters of single-domain magnetite contained in natural plagioclase crystal. *Geophys J Int* 202:394–401. <https://doi.org/10.1093/gji/ggv154>
- Sato M, Kimura Y, Tanaka S, Hatakeyama T, Sugita S, Nakamura T, Tachibana S, Yurimoto H, Noguchi T, Okazaki R, Yabuta H, Naraoka H, Sakamoto K, Yada T, Nishimura M, Nakato A, Miyazaki A, Yogata K, Abe M, Okada T, Usui T, Yoshikawa M, Saiki T, Terui F, Nakazawa S, Watanabe S, Tsuda Y (2022) Rock magnetic characterization of returned samples from asteroid (162173) Ryugu: implications for paleomagnetic interpretation and paleointensity estimation. *J Geophys Res Planet* 127(11):e2022JE007405. <https://doi.org/10.1029/2022JE007405>
- Selkin PA, Gee JS, Tauxe L (2007) Nonlinear thermoremanence acquisition and implications for paleointensity data. *Earth Planet Sci Lett* 256:81–89. <https://doi.org/10.1016/j.epsl.2007.01.017>
- Shcherbakova VV, Bakhmutov VG, Thallner D, Shcherbakov VP, Zhidkov GV, Biggin AJ (2020) Ultra-low palaeointensities from East European Craton, Ukraine support a globally anomalous palaeomagnetic field in the Ekiacaran. *Geophys J Int* 220:1928–1946. <https://doi.org/10.1093/gji/ggg2566>
- Smirnov AV, Tarduno JA (2005) Thermochemical remanent magnetization in Precambrian rocks: Are we sure the geomagnetic field was weak? *J Geophys Res Solid Earth* 110:B06103. <https://doi.org/10.1029/2004J8003445>
- Smirnov AV, Tarduno JA, Pisakin BN (2003) Paleointensity of the early geodynamo (2.45 Ga) as recorded in Karelia: A single-crystal approach. *Geology* 31(5):415–418. [https://doi.org/10.1130/0091-7613\(2003\)031%3c0415:POTEGG%3e2.0.CO;2](https://doi.org/10.1130/0091-7613(2003)031%3c0415:POTEGG%3e2.0.CO;2)
- Stevenson DJ, Spohn T, Schubert G (1983) Magnetism and thermal evolution of the terrestrial planets. *Icarus* 54(3):466–489. [https://doi.org/10.1016/0019-1035\(83\)90241-5](https://doi.org/10.1016/0019-1035(83)90241-5)
- Stöhr J (1999) Exploring the microscopic origin of magnetic anisotropies with X-ray magnetic circular dichroism (XMCD) spectroscopy. *J Magn Magn Mater* 200:470–497. [https://doi.org/10.1016/S0304-8853\(99\)00407-2](https://doi.org/10.1016/S0304-8853(99)00407-2)
- Sugawara T (2001) Ferric iron partitioning between plagioclase and silicate liquid: thermodynamics and petrological applications. *Contrib Mineral Petrol* 141:639–686. <https://doi.org/10.1007/s004100100267>
- Takahashi F, Tsunakawa H, Matsushima M, Mochizuki N, Honkura Y (2008) Effects of thermally heterogeneous structure in the lowermost mantle on the geomagnetic field strength. *Earth Planet Sci Lett* 272(3):738–746. <https://doi.org/10.1016/j.epsl.2008.06.017>
- Tang F, Taylor RJM, Einsle JF, Borlina CS, Fu RR, Weiss BP, Williams HM, Williams W, Nagy L, Midgley PA, Lima EA, Bell EA, Harrison TM, Alexander EW, Harrison RJ (2019) Secondary magnetite in ancient zircon precludes analysis of a Hadean geodynamo. *Proc Natl Acad Sci* 116(2):407–412. <https://doi.org/10.1073/pnas.1811074116>
- Tani K, Dunkley DJ, Kimura J, Wysoczanski RJ, Yamada K, Tatsumi Y (2010) Syncollisional rapid granitic magma formation in an arc–arc collision zone: evidence from the Tanzawa plutonic complex, Japan. *Geology* 38:215–218. <https://doi.org/10.1130/G30526.1>
- Tarduno JA (2009) Geodynamo history preserved in single silicate crystals: origins and long-term mantle control. *Elements* 5(4):217–222. <https://doi.org/10.2113/gselements.5.4.217>
- Tarduno JA, Cottrell RD (2005) Dipole strength and variation of the time-averaged reversing and nonreversing geodynamo based on Thellier analyses of single plagioclase crystals. *J Geophys Res Solid Earth* 110:B11101. <https://doi.org/10.1029/2005JB003970>
- Tarduno JA, Cottrell RD (2013) Signals from the ancient geodynamo: A paleomagnetic field test on the Jack Hills metaconglomerate. *Earth Planet Sci Lett* 367:123–132. <https://doi.org/10.1016/j.epsl.2013.02.008>
- Tarduno JA, Cottrell RD, Smirnov AV (2001) High geomagnetic intensity during the mid-Cretaceous from Thellier analyses of single plagioclase crystals. *Science* 291:1779–1783. <https://doi.org/10.1126/science.1057519>
- Tarduno JA, Cottrell RD, Smirnov AV (2002) The Cretaceous superchron geodynamo: Observations near the tangent cylinder. *Proc Natl Acad Sci* 99(22):14020–14025. <https://doi.org/10.1073/pnas.222373499>
- Tarduno JA, Smirnov AV (2004) The paradox of low field values and the long-term history of the geodynamo. In: Channell JET et al. (eds) *Timescales of the paleomagnetic field*, geophys monogr ser, vol 145. AGU, Washington DC, pp 75–84
- Tarduno JA, Cottrell RD, Smirnov AV (2006) The paleomagnetism of single silicate crystals: Recording geomagnetic field strength during mixed polarity intervals, superchrons, and inner core growth. *Rev Geophys* 44(1):RG1002. <https://doi.org/10.1029/2005RG000189>
- Tarduno JA, Cottrell RD, Watkeys MK, Bauch D (2007) Geomagnetic field strength 3.2 billion years ago recorded by single silicate crystals. *Nature* 446(7136):657–660. <https://doi.org/10.1038/nature05667>
- Tarduno JA, Cottrell RD, Watkeys MK, Hofmann A, Dourovine PV, Mama-jek EE, Liu D, Sibeck DG, Neukirch LP, Usui Y (2010) Geodynamo, solar wind, and magnetopause 3.4 to 3.45 billion years ago. *Science* 327(5970):1238–1240. <https://doi.org/10.1126/science.1183445>
- Tarduno JA, Cottrell RD, Nimmo F, Hopkins J, Voronov J, Erickson A, Blackman E, Scott ERD, McKinley R (2012) Evidence for a dynamo in the main group pallisite parent body. *Science* 338:939–942. <https://doi.org/10.1126/science.1223932>

- Tarduno JA, Blackman EG, Mamajek EE (2014) Detecting the oldest geodynamo and attendant shielding from the solar wind: Implications for habitability. *Phys Earth Planet Inter* 233:68–87. <https://doi.org/10.1016/j.pepi.2014.05.007>
- Tarduno JA, Cottrell RD, Davis WJ, Nimmo F, Bono RK (2015) A Hadean to Paleoproterozoic geodynamo recorded by single zircon crystals. *Science* 349(6247):521–524. <https://doi.org/10.1126/science.1261114>
- Tarduno JA, Cottrell RD, Bono RK, Oda H, Davis WJ, Fayek M, van't Erve O, Nimmo F, Huang W, Thern ER, Fearn S, Mitra G, Smirnov AV, Blackman EG (2020) Paleomagnetism indicates that primary magnetite in zircon records a strong Hadean geodynamo. *Proc Natl Acad Sci* 117(5):2309–2318. <https://doi.org/10.1073/pnas.1916553117>
- Tarduno JA, Cottrell RD, Lawrence K, Bono RK, Huang W, Johnson CL, Blackman EG, Smirnov AV, Nakajima M, Neal CR, Zhou T, Ibanez-Mejia M, Oda H, Crummins B (2021) Absence of a long-lived lunar paleomagnetosphere. *Sci Adv* 7(32):7647. <https://doi.org/10.1126/sciadv.abi7647>
- Tarduno JA, Cottrell RD, Bono RK, Rayner N, Davis WJ, Zhou T, Nimmo F, Hofmann A, Jodder J, Ibanez-Mejia M, Watkeys MK, Oda H, Mitra G (2023) Hadaean to Palaeoproterozoic stagnant-lid tectonics revealed by zircon magnetism. *Nature* 618:531–536. <https://doi.org/10.1038/s41586-023-06024-5>
- Tauxe L, Staudigel H (2004) Strength of the geomagnetic field in the Cretaceous Normal Superchron: New data from submarine basaltic glass of the Troodos Ophiolite. *Geochem Geophys Geosyst* 5(2):Q02H06. <https://doi.org/10.1029/2003GC000635>
- Taylor RJM, Reddy SM, Saxey DW, Rickard WDA, Tang F, Borlina CS, Fu RR, Weiss BP, Bagot P, Williams HM, Harrison RJ (2023) Direct age constraints on the magnetism of Jack Hills zircon. *Sci Adv* 9(1):eadd1511. <https://doi.org/10.1126/sciadv.add1511>
- Thallner D, Biggin AJ, Halls HC (2021a) An extended period of extremely weak geomagnetic field suggested by palaeointensities from the Ediacaran Grenville dykes (SE Canada). *Earth Planet Sci Lett* 568:117025. <https://doi.org/10.1016/j.epsl.2021.117025>
- Thallner D, Biggin AJ, McCausland PJA, Fu RR (2021b) New paleointensities from the Skinner Cove Formation, Newfoundland, suggest a changing state of the geomagnetic field at the Ediacaran-Cambrian transition. *J Geophys Res Solid Earth* 126:e2021JB022292. <https://doi.org/10.1029/2021JB022292>
- Thallner D, Shcherbakova VV, Bakmutov VG, Shcherbakov VP, Zhidkov GV, Poliachenko IB, Biggin AJ (2022) New palaeodirections and palaeointensity data from extensive profiles through the Ediacaran section of the Volyn Basalt Province (NW Ukraine). *Geophys J Int* 231:474–492. <https://doi.org/10.1093/gji/ggac186>
- Thellier E, Thellier O (1959) Sur l'intensité du champ magnétique terrestre dans le pass historique et géologique. *Ann Geophys* 15:285–376
- Tsunakawa H, Shaw J (1994) The Shaw method of palaeointensity determinations and its application to recent volcanic rocks. *Geophys J Int* 118:781–787. <https://doi.org/10.1111/j.1365-246X.1994.tb03999.x>
- Tsunakawa H, Wakabayashi KI, Mochizuki N, Yamamoto Y, Ishizaka K, Hirata T, Takahashi F, Seita K (2009) Paleointensity study of the middle Cretaceous Iritono granite in northeast Japan: Implication for high field intensity of the Cretaceous normal superchron. *Phys Earth Planet Int* 176(3):235–242. <https://doi.org/10.1016/j.pepi.2009.07.001>
- Usui Y (2013) Paleointensity estimates from oceanic gabbros: Effects of hydrothermal alteration and cooling rate. *Earth Planet Space* 65:985–996. <https://doi.org/10.5047/eps.2013.03.015>
- Usui Y, Nakamura N (2009) Nonlinear thermoremanence corrections for Thellier paleointensity experiments on single plagioclase crystals with exsolved magnetites: a case study for the Cretaceous Normal Superchron. *Earth Planet Space* 61:1327–1337. <https://doi.org/10.1186/BF03352985>
- Usui Y, Tian W (2017) Paleomagnetic directional groups and paleointensity from the flood basalt in the Tarim large igneous province: implications for eruption frequency. *Earth Planet Space* 69:14. <https://doi.org/10.1186/s40623-016-0595-x>
- Usui Y, Tarduno JA, Watkeys MK, Hofmann A, Cottrell RD (2009) Evidence for a 3.45-billion-year-old magnetic remanence: Hints of an ancient geodynamo from conglomerates of South Africa. *Geochem Geophys Geosyst* 10:Q09Z07. <https://doi.org/10.1029/2009GC002496>
- Usui Y, Shibuya T, Sawaki Y, Komiya T (2015) Rock magnetism of tiny exsolved magnetite in plagioclase from a Paleoproterozoic granitoid in the Pilbara craton. *Geochem Geophys Geosyst* 16:112–125. <https://doi.org/10.1002/2014GC005508>
- Usui Y, Shimono T, Yamazaki T (2018) Rock magnetism of quartz and feldspars chemically separated from pelagic red clay: a new approach to provenance study. *Earth Planet Space* 70:153. <https://doi.org/10.1186/s40623-018-0918-1>
- van der Laan G (2013) Applications of soft X-ray magnetic dichroism. *J Phys Conf Ser* 430:012127. <https://doi.org/10.1088/1742-6596/430/1/012127>
- Veitch RJ, Hedley IG, Wagner JJ (1984) An investigation of the intensity of the geomagnetic field during Roman times using magnetically anisotropic bricks and tiles. *Arch Sci* 37:359–373
- Wakabayashi KI, Tsunakawa H, Mochizuki N, Yamamoto Y, Takigami Y (2006) Paleomagnetism of the middle Cretaceous Iritono granite in the Abukuma region, northeast Japan. *Tectonophysics* 421:161–171. <https://doi.org/10.1016/j.tecto.2006.04.013>
- Weiss BP, Lima EA, Fong LE, Baudenbacher FJ (2007) Paleointensity of the Earth's magnetic field using SQUID microscopy. *Earth Planet Sci Lett* 264(1–2):61–71. <https://doi.org/10.1016/j.epsl.2007.08.038>
- Weiss BP, Maloof AC, Tailby N, Ramezani J, Fu RR, Hanus V, Trail D, Watson EB, Harrison TM, Bowring SA, Kirschvink JL, Swanson-Hysell NL, Coe RS (2015) Pervasive remagnetization of detrital zircon host rocks in the Jack hills, Western Australia and implications for records of the early geodynamo. *Earth Planet Sci Lett* 430:115–128. <https://doi.org/10.1016/j.epsl.2015.07.067>
- Weiss BP, Fu RR, Einsle JF, Glenn DR, Kehayias P, Bell EA, Gelb J, Araujo JFDF, Lima EA, Borlina CS et al (2018) Secondary magnetic inclusions in detrital zircons from the Jack Hills, Western Australia, and implications for the origin of the geodynamo. *Geology* 46(5):427–430. <https://doi.org/10.1130/G39938.1>
- Wenk HR, Chen K, Smith R (2011) Morphology and microstructure of magnetite and ilmenite inclusions in plagioclase from Adirondack anorthositic gneiss. *Am Miner* 96(8–9):1316–1324. <https://doi.org/10.2138/am.2011.3760>
- Windmill RJ, Franchi IA, Hellmann JL, Schneider JM, Spitzer F, Kleine T, Greenwood RC, Anand M (2022) Isotopic evidence for palasite formation by impact mixing of olivine and metal during the first 10 million years of the Solar System. *Proc Natl Acad Sci Nexus* 1:1–11. <https://doi.org/10.1093/pnasnexus/pgac015>
- Yamamoto Y, Tsunakawa H (2005) Geomagnetic field intensity during the last 5 Myr: LTD-DHT Shaw palaeointensities from volcanic rocks of the Society Islands, French Polynesia. *Geophys J Int* 162(1):79–114. <https://doi.org/10.1111/j.1365-246X.2005.02651.x>
- Yamamoto Y, Tsunakawa H, Shibuya H (2003) Palaeointensity study of the Hawaiian 1960 lava: Implications for possible causes of erroneously high intensities. *Geophys J Int* 153(1):263–276. <https://doi.org/10.1046/j.1365-246x.2003.01909.x>
- Yamamoto Y, Torii M, Natsuhara N (2015) Archeointensity study on baked clay samples taken from the reconstructed ancient kiln: implication for validity of the Tsunakawa-Shaw paleointensity method. *Earth Planets Space* 67:63. <https://doi.org/10.1186/s40623-015-0229-8>
- Yu Y (2011) Importance of cooling rate dependence of thermoremanence in paleointensity determination. *J Geophys Res Solid Earth* 116:B09101. <https://doi.org/10.1029/2011JB008388>
- Yu Y, Dunlop DJ (2003) On partial thermoremanent magnetization tail checks in Thellier paleointensity determination. *J Geophys Res Solid Earth* 108(B11):2523. <https://doi.org/10.1029/2003JB002420>
- Yu Y, Tauxe L, Genevey A (2004) Toward an optimal geomagnetic field intensity determination technique. *Geochem Geophys Geosyst* 5(2):07. <https://doi.org/10.1029/2003GC000630>
- Zhou T, Tarduno JA, Nimmo F, Cottrell RD, Bono RK, Ibanez-Mejia M, Huang W, Hamilton M, Kodama K, Smirnov AV, Crummins B, Padgett F (2022) Early Cambrian renewal of the geodynamo and the origin of the inner core structure. *Nat Comm* 13:4161. <https://doi.org/10.1038/s41467-022-31677-7>

Publisher's Note

Springer Nature remains neutral with regard to jurisdictional claims in published maps and institutional affiliations.